AD NUMBER

AD882199

LIMITATION CHANGES

TO:

Approved for public release; distribution is unlimited.

FROM:

Distribution authorized to U.S. Gov't. agencies only; Test and Evaluation; APR 1971. Other requests shall be referred to Arnold Engineering Development Center, Arnold ADB, TN.

AUTHORITY

AEDC ltr 30 Aug 1984

AEDC-TR-71-68

cy 6

RECOVERY CHARACTERISTICS OF A SINGLE-SHIELDED SELF-ASPIRATING THERMOCOUPLE PROBE AT LOW PRESSURE LEVELS AND SUBSONIC SPEEDS

C. E. Willbanks

ARO, Inc.

April 1971

ENGINE TEST FACILITY

ARNOLD ENGINEERING DEVELOPMENT CENTER

AIR FORCE SYSTEMS COMMAND

ARNOLD AIR FORCE STATION, TENNESSEE

NOTICES

When U. S. Government drawings specifications, or other data are used for any purpose other than a definitely related Government procurement operation, the Government thereby incurs no responsibility nor any obligation whatsoever, and the fact that the Government may have formulated, furnished, or in any way supplied the said drawings, specifications, or other data, is not to be regarded by implication or otherwise, or in any manner licensing the holder or any other person or corporation, or conveying any rights or permission to manufacture, use, or sell any patented invention that may in any way be related thereto.

Qualified users may obtain copies of this report from the Defense Documentation Center.

References to named commercial products in this report are not to be considered in any sense as an endorsement of the product by the United States Air Force or the Government.

RECOVERY CHARACTERISTICS OF A SINGLE-SHIELDED SELF-ASPIRATING THERMOCOUPLE PROBE AT LOW PRESSURE LEVELS AND SUBSONIC SPEEDS

C. E. Willbanks
ARO, Inc.

FOREWORD

The work reported herein was sponsored by the Air Force Aerospace Propulsion Laboratory, Air Force Systems Command (AFSC), Wright-Patterson Air Force Base, Ohio, under Program Element 65401F.

The results of the research presented were obtained by ARO, Inc. (a subsidiary of Sverdrup & Parcel and Associates, Inc.), contract operator of AEDC, AFSC, under Contract F40600-71-C-0002. The research was conducted from September 1968 to June 1970 under ARO Project Numbers RD0953 and RD0850, and the manuscript was submitted for publication on February 4, 1971.

This technical report has been reviewed and is approved.

Walter C. Knapp
Lt Colonel, USAF
AF Representative, ETF
Directorate of Test

Joseph R. Henry
Colonel, USAF
Director of Test

ABSTRACT

An apparatus which produces a well-defined flow field for calibration of thermocouple probes over a wide range of subsonic flow conditions at low pressure levels is described. Results for calibration of a typical thermocouple probe used in engine testing are presented. Temperature recovery characteristics are presented for a thermocouple probe of the single-shielded, self-aspirating type for total pressures of 0.75, 1.0, 3.0, 7.5, and 15 psia with subsonic flow speeds ranging from Mach number 0.25 to Mach number 1.0. The total temperature of the air was approximately 670°R for all the tests. An analysis of the probe recovery characteristics based on a semi-empirical correlation was made, and the correlation appears to give satisfactory results over the entire Mach number and total pressure range considered.

CONTENTS

APPENDIXES

I. ILLUSTRATIONS

Figure

NOMENCLATURE

A_F	Surface area of fin per tube per fin, ft^2
A_s	Internal cross sectional area of probe shield, ft^2
A_T	Nozzle throat area, $in.^2$
A_v	Total area of vent holes in probe, ft^2
C_D	Discharge coefficient for vent holes
C_p	Specific heat of air at constant pressure, Btu/lbm°R

D_i	Inside diameter of heat exchanger tube, in.
D_o	Outside diameter of heat exchanger tube, in.
G	Rate of mass flow through heat exchanger, lbm/hr
H	Cooled length of tube, ft
$\bar{h}$	Effective heat transfer coefficient for thermocouple, Btu/hr-ft^2-°F
h_F	Heat transfer coefficient for the fins on the air side, Btu/hr-ft^2-°F
h_S	Heat transfer for steam condensing inside tubes, Btu/hr-ft^2-°F
h_T	Heat transfer coefficient for tube, Btu/hr-ft^2-°F
$\bar{k}$	Effective thermal conductivity of thermocouple leads, Btu/hr-ft-°F
k_a	Thermal conductivity of air, Btu/hr-ft-°F
k_T	Thermal conductivity of tube, Btu/hr-ft-°F
L	Effective length of heat exchanger, ft
$\bar{\ell}$	Characteristic dimension of thermocouple, ft
M	Mach number in test section
M_s	Mach number of flow inside probe shield
Nu_I	Nusselt number index
Pr	Prandtl number
p	Static pressure, psia
p_o	Total pressure, psia
Δp	Static pressure across the nozzle, psi
Q	Rate of heat transfer, Btu/hr
R	Gas constant for air, appropriate units
S	Fin spacing, in.
T	Static temperature of gas, °R
T_{b1}	Bulk temperature of air entering the heat exchanger, °R
T_{b2}	Bulk temperature of air leaving the heat exchanger, °R
T_H	Temperature of heat exchanger core, °R
T_o	Total temperature, °R

T_{p_a}	Adiabatic probe temperature or adiabatic recovery temperature, °R
T_s	Saturated steam temperature, °R
T_{TB}	Temperature at base of thermocouple where it enters stem, °R
t	Fin thickness, in.
U_F	Overall heat transfer coefficient for fins, Btu/hr-ft^2-°F
U_T	Overall heat transfer coefficient for tubes, Btu/hr-ft^2-°F
W_F	Fin area per unit length of heat exchanger, ft
W_T	Tube area per unit length of heat exchanger, ft
x	Distance along heat exchanger, ft
α	Constant at proportionality
γ	Ratio of specific heat for air
Δ	Recovery-temperature correction factor
η_F	Fin efficiency
μ_a	Viscosity of air, lbf/sec/ft^2

SECTION I
INTRODUCTION

The temperature indicated by a thermocouple probe is governed by a balance between the net rate of heat transfer and rate of energy storage at the thermocouple junction. Heat transfer may occur by the convection, radiation, and conduction modes. The relative importance of these modes of heat transfer depends in large measure on probe design. In the absence of heat exchange between a probe and its environment, a thermocouple probe usually indicates a temperature which lies between the static temperature and total temperature of the stream in which it is immersed. This indicated temperature is called the adiabatic probe temperature or recovery temperature of the probe. The difference between static and total temperature is $\left(\frac{\gamma - 1}{2} M^2\right)T$. Thus, it is necessary to know the relationship of the recovery temperature to static temperature if the error in temperature is to be kept below $\left(\frac{\gamma - 1}{2} M^2\right)T$. Radiation and conduction heat transfer to a probe is not always negligible, and frequently, corrections must be applied to the probe indicated temperature before the recovery temperature, and finally the true gas temperature, can be obtained.

The relationship of recovery temperature to total temperature for a probe depends on probe geometry, the material from which the probe is constructed, probe orientation relative to the flow direction, type of fluid, the fluid velocity, and the thermodynamic state of the fluid itself. In almost all cases, this relationship must be determined experimentally. The experimental approach is to immerse a particular probe in a well-defined flow field and to compare the recovery temperature of the probe with the total temperature of the fluid. By exposing the probe to a sufficiently wide range of flow conditions, its recovery characteristics can be determined as a function of the velocity and thermodynamic state of the fluid.

One of the problems associated with this experimental approach is the accurate determination of the total temperature of the fluid in the calibration apparatus. Usually the total temperature is measured directly with a thermocouple in a region of the flow field where the fluid velocity is low. This technique becomes increasingly less reliable as the gas density is reduced since stem conduction and radiation heat transfer effects become of greater importance relative to the convective heat transfer in establishing the thermocouple temperature. The apparatus used in this study circumvents the difficult problem of direct

measurement of the fluid temperature in the apparatus. In the apparatus, air is heated at low velocity in an indirect heat exchanger having a large amount of surface area and employing saturated steam as an isothermal heat source. After being heated to very near the steam temperature, the air is accelerated in a nozzle to the desired Mach number. The total temperature of the fluid stream is, therefore, nearly equal to the temperature of the heat exchanger core which can be readily measured. The apparatus is well suited for calibration of probes at low gas densities corresponding to high altitude flight conditions.

Figures 1a and b (Appendix I) show a sketch and a photograph of a typical thermocouple probe configuration for use in turbojet engine testing. This probe is self aspirating since the flow around the probe shield induces flow through the shield and around the thermocouple junction. In the present study, recovery temperature characteristics of three probes of this configuration (Fig. 1a) were determined over a wide range of subsonic flow conditions. Saturated steam at atmospheric pressure was used as a heat source; therefore, all of the tests were conducted at approximately 210°F total temperature.

No attempt is made here to present a comprehensive survey of the literature on thermocouple probes. Rather, the survey is confined primarily to those studies considering probe recovery temperature characteristics at low pressures in subsonic flow, i. e., characteristics at low Reynolds numbers, and those studies on thermocouple probes of the self-aspirating type since these are the areas of primary interest in the present investigation.

Hottel and Kalitinsky (Ref. 1) presented the results of an investigation of temperature measurements in high velocity air streams. Three types of self-aspirating probes as well as bare wire thermocouples were investigated. The parameters affecting thermocouple behavior in a gas stream were noted. Importance of probe vent area and thermocouple location for the so-called Franz probe was shown, and temperature recovery and radiation characteristics were determined for two other self-aspirating types of thermocouple probes.

The results of a theoretical and experimental study of thermocouple probe recovery temperature characteristics is presented in Ref. 2 by Malmquist. In this study, it was found that there exists an optimum vent hole area-to-internal shield cross-sectional area ratio for maximum probe temperature recovery, and the importance of locating the thermocouple junction ahead of the vent holes was shown. Malmquist also determined that the material from which a probe is constructed has an influence on its recovery characteristics. The experiments were conducted at a total temperature near 80°F and a static pressure of one atmosphere.

Considerable research effort was devoted to the investigation and development of thermocouple probes by NACA. Two reports on this research are particularly pertinent to the present study. Stickney (Ref. 3) reported time constants and temperature recovery characteristics for six thermocouple probes. Data were presented for a total temperature of approximately 80°F for both subsonic and supersonic Mach numbers and over the total pressure range from 0.2 to 2.3 atm. Glawe, Simmons, and Stickney (Ref. 4) presented results of an experimental study of thermal radiation and recovery characteristics as well as time constants for nine probes. Total pressures of 0.2, 0.5, and 1.0 atm, Mach numbers of 0.3, 0.6, and 0.9, and a total temperature of approximately 80°F were the test conditions in the determination of recovery temperature characteristics. One of the probes tested is similar to the probe investigated in this study. In order that these two probes may be compared and contrasted, they are shown in Fig. 1.

In all of the previously mentioned studies, the stagnation temperature of the gas stream was determined through direct measurement in each calibration apparatus.

SECTION II
APPARATUS

The arrangement of the experimental apparatus used in the investigation is shown in Fig. 2. It is connected to the Engine Test Facility (ETF) air supply and exhaust plant. This apparatus is capable of providing air within a fraction of a degree of the saturation temperature of steam at ambient pressure. In the test section, velocities up to sonic velocity and total pressures from 0.75 to 15 psia can be provided.

2.1 TEST CELL

The heart of the apparatus is the heat exchanger, a photograph of which is shown in Fig. 3. Appendix III presents an analysis of the performance of the heat exchanger which gives the temperature rise of the air through the exchanger as a function of flow rate. After flowing through the heat exchanger, the air enters a converging nozzle where it is accelerated to the desired Mach number. The flow from the nozzle forms a free jet, and the test section is taken to be one inch downstream of the nozzle lip which is well within the potential core of the jet. The Mach number in the test section is calculated from the isentropic flow relations and the pressure ratio across the nozzle. The pressure ratio

across the nozzle was determined from the plenum pressure and the static pressure at the wall of the exhaust duct at a location coincident with the nozzle exit plane. This implies the assumption of uniform static pressure across the exhaust duct in the neighborhood of the nozzle exit plane.

As indicated in Fig. 2, the saturated steam is generated by boiling water in the bottom of the steam jacket. Heat to boil the water is obtained by passing steam from the steam plant through copper coils immersed in the water. The saturated vapor is forced to flow up vertically through the tubes in the heat exchanger and along the steam jacket where it surrounds the exhaust duct and nozzle flange. It exhausts into the laboratory at ambient pressure. The passages for flow of steam are large, and flow velocities are low; therefore, the pressure inside the steam jacket of the apparatus is virtually uniform at ambient pressure. Since the steam is saturated, the pressure determines its temperature; hence, the steam temperature is uniform inside the apparatus.

The nominal exit diameter of the nozzle is four inches. The plenum-to-nozzle area ratio is 11.4, which gives a maximum Mach number of 0.05 in the plenum. Thus, the plenum can be considered to be a stagnation chamber, and the total temperature can be taken to be equal to the temperature of the air at the exit of the heat exchanger.

Pressures in the apparatus were measured with a combination of gages and differential manometers apropos the test conditions.

The temperatures were measured with copper-constantan thermocouples. The electrical circuit for the thermocouple is shown schematically in Fig. 4. The electromotive force (emf) output for the thermocouples was measured with a potentiometer in a bridge circuit utilizing an external electronic galvanometer to indicate a null condition for the circuit. From Fig. 4, it can be noted that the thermocouples in the probes are referenced to a thermocouple junction mounted on the heat exchanger.

2.2 TEST ARTICLE

A sketch of the thermocouple probe which was tested is shown in Fig. 1a. A photograph of the probe is presented in Fig. 1b. Three probes were tested simultaneously by installing the probes in a rake. The rake was mounted so that the center probe was on the centerline of the nozzle. The other two probes were positioned 0.75 in. above and below the centerline. All of the probes were located approximately one inch downstream of the nozzle lip. The probes were fabricated from

stainless steel tubing (Types 303 and 304), and the thermocouples in the probes were copper-constantan. Equality of aspiration rates for the three probes, at least for high Reynolds number, was verified by comparing the rates of flow through the shields in a direct-connect test. One end of a piece of plastic tubing, whose other end was connected to a nitrogen gas bottle, was fitted to the front end of a probe shield with the vent holes in the probe being left open to the atmosphere. Thus, nitrogen could flow from the bottle through the tubing and through the shield and finally be exhausted to the atmosphere through the vent holes. The bottle was pressurized with nitrogen, and the time required for the pressure in the bottle to drop a given amount was noted. This was repeated for each of the three probes. The times for the three probes were found to agree satisfactorily, thus indicating equality of aspiration rates at high Reynolds number.

It is worthy to note that considerable difficulty was experienced with foreign particles becoming lodged in the vent holes of the probes during testing. Usually there was a discernible decrease in the recovery temperature for the probe when this happened. It was necessary to remove the rake from the cell and clean the probes when such a change was noted.

Early in the study, difficulties were also experienced with stem leakage because of the large pressure difference across the stem. This problem was solved by redesigning the probe rake.

SECTION III
RESULTS AND DISCUSSION

The recovery temperature characteristics of three probes were determined at a total temperature of 670°R and total pressures of 0.75, 1.0, 3.0, 7.5, and 15.0 psia over a Mach number range from 0.25 to 1.0. Table I (Appendix II) presents the results of the calibration in the form of the correction factor Δ which is defined as

$$\Delta = \frac{T_o - T_{p_a}}{T_o}$$

The average recovery correction factor for the three probes tested is shown graphically as a function of Mach number and pressure level in Fig. 5. Also shown in this figure are recovery correction factor curves as predicted by the semi-empirical correlation developed in Appendix IV. Figure 6 shows smooth curves which fit the average recovery correction factor data given in Fig. 5. The cross-hatched regions represent the

spread in data for all three probes tested, after smoothing. Most all of the individual data points for the three probes lie within the cross-hatched regions.

From Fig. 5, it is evident that the recovery correction factor increases with Mach number and decreasing total pressure level. It was found that generally the recovery correction factor for Probes 2 and 3 showed close agreement, whereas Probe 1 gave a slightly lower recovery correction factor than did Probes 2 and 3. Variation among the three probes is believed to be due to differences in probe construction. It should be noted that the magnitude of the variation among probes is about the same as the variation observed by Stickney (Ref. 3) and Glawe, Simmons, and Stickney (Ref. 4).

Also shown in Figs. 6c, d, and e are the data obtained by Glawe, Simmons, and Stickney with the probe shown in Fig. 1c. Clearly there is considerable difference in the NACA data and the data obtained in the present study. This is not too surprising in view of the differences in probe design and construction materials. Apparently, heat conduction through the thermocouple leads to the thermocouple junction plays an important role in recovery characteristics of the thermocouple probe, and the effective thermal conductivity of copper-constantan thermocouple leads is much greater than the effective thermal conductivity of Chromel®-Alumel® thermocouple leads. Moreover, the NACA probe is about twice as large as the probe of the present study and has a much different vent hole to internal shield area ratio.

In Appendix IV, a simplified analysis of the self-aspirating type of probe is presented. The analysis shows that the temperature recovery correction can be correlated in terms of free-stream Mach number and a Nusselt number index for the thermocouple inside the shield. The results of the correlation are shown in Figs. 7, 8, and 9. To use the correlation, the Nusselt number index

$$Nu_I = 1.1 \times 10^4 \, k_a \sqrt[3]{Pr} \sqrt{\frac{\gamma p_o M_s}{\sqrt{\gamma R T_o}\, \mu_a}}$$

is computed using Fig. 7 to estimate the Mach number of the flow past the thermocouple junction. For air in the temperature range from 400 to 700°R, $Nu_I = \sqrt{p_o M_s}$ where p_o is in psia. From the Nusselt number index, the corresponding value of Δ/Δ_{ref} is obtained from Fig. 8. The value of Δ_{ref} is determined from Fig. 9 at the free-stream Mach number. Finally, the recovery correction Δ is determined from the product $(\Delta_{ref})(\Delta/\Delta_{ref})$. The dashed lines in Fig. 5 were determined from this

correlation method. The correlation is seen to be reasonably good over the entire Mach number and pressure range considered.

Although the correlation cannot be used to predict the effect of changing probe geometry or size on recovery temperature correction, it can be used to predict the effect of changing the gas temperature and composition. This is discussed in Appendix IV.

SECTION IV
EXPERIMENTAL ERROR AND ACCURACY OF THE RESULTS

In this section, the various sources of experimental errors and their effects on the results are discussed.

The recovery temperature correction factor is defined as

$$\Delta = \frac{T_o - T_{p_a}}{T_o}$$

The temperatures (T_o and T_{p_a}) are not measured directly but rather are inferred from the measured quantities, T_H and ($T_H - T_{p_a}$). Since the heat exchanger is always heating the air, it follows that T_o is less than T_H and T_H is less than T_S, although hopefully all three temperatures are very close together. In Appendix III, the maximum difference between T_o and T_S is determined as a function of total pressure and Mach numbers in the test section. From the analysis, it follows that

$$T_H - T_o < (T_s - T_{b_1}) \exp(-28800/G)$$

where G is the rate of mass flow through the heat exchanger in pounds per hour. It can be shown that for isentropic flow through the nozzle

$$G = p_o A_T \sqrt{\frac{\gamma}{RT_{b_2}}} \frac{M}{\left[1 + \frac{\gamma - 1}{2} M^2\right]^{(\gamma+1)/2(\gamma-1)}}$$

For $p_o \leq 3.0$ psia, the difference between the steam and entering air temperature ($T_S - T_{b_1}$) was less than 140°F.[1] By preheating the air, $T_S - T_{b_1}$ was kept below 40°F for the data obtained at 7.5 and 15 psia.

---

[1]With this temperature difference, the air leaves within 0.05°F of the steam temperature when $p_o \leq 3.0$ psia.

This difference is a fixed or systematic error which arises because of uncertainty in performance or efficiency of the heat exchanger. That is, the temperature of the air leaving the heat exchanger is not known exactly. It is only known that it must be less than the steam temperature and must be greater than the temperature predicted by the somewhat conservative analysis of Appendix III. In addition to this uncertainty, there are errors associated with the measurement of T_H and $T_H - T_{p_a}$. There are three primary sources of error in these quantities.

The temperatures were determined from thermocouples using the appropriate standard thermocouple tables without correction. A single point calibration of all the thermocouples between the ice point and boiling point for one atmosphere showed that the temperature difference given by the thermocouple was within 1.25°F out of 178°F in T_H, and if the error is assumed to vary linearly with temperature difference, it results in an error of $0.007 (T_H - T_{p_a})$ in $T_H - T_{p_a}$. This error is consistent with the limits of error given by manufacturers for thermocouples fabricated from "off the shelf" thermocouple wire.

The potentiometer used to measure the output of the thermocouple was calibrated against a precision voltage source. The indicated emf of the potentiometer was found to agree with the actual emf within 2.5 μv (0.1°F for the copper-constantan thermocouple system) over the range needed to measure $T_H - T_{p_a}$. Agreement was within 5.0 μv (0.2°F) over the range needed to measure T_H with respect to an ice bath at 32°F.

In an attempt to minimize the error of observation, three readings were taken at each test condition. Deviation of individual readings from the average was less than ±3 μv (0.12°F) for almost all data points. By using the method of least squares, the probable error of observation, based on a probability of 1/2 that an error taken at random will be greater or less than the probable error, was found to be less than 1.5 μv or 0.06°F for virtually all data points.

The Mach number of the flow in the test section was determined from the isentropic flow relationship

$$M = \sqrt{\frac{2}{\gamma - 1}\left[\left(1 - \frac{\Delta p}{p_o}\right)^{(1-\gamma)/\gamma} - 1\right]}$$

where the total pressure (p_o) and the pressure difference (Δp) across the nozzle were measured. Since there are errors in the measurement of p_o and Δp, there is a corresponding error in Mach number. The gages used in measuring p_o and Δp were calibrated, and the maximum error in

calculating the Mach number from the above equation including the observational error is estimated to be less than ±0.005 Mach number. This error in Mach number can be converted to an error in Δ by taking the product of the slope dΔ/dM with the error in M, namely ±0.005. For the present purpose, it is sufficiently accurate to take $\Delta \propto M^2$, which leads to an additional error in Δ of approximately ±0.001 Δ/M.

If it is assumed that the errors are additive, it follows that

$$\Delta = \frac{(T_H - T_{p_a})_I}{(T_H)_I}$$

with a maximum positive error of

$$(9.3\Delta + \Delta/M + 0.236)/1000$$

and a maximum negative error of

$$(9.3\Delta + \Delta/M + 0.236)/1000 + \frac{T_s - T_{b_I}}{T_s} \exp\left(-\frac{28800}{G}\right)$$

where the subscript I denotes the average indicated values of T_H and $T_H - T_{p_a}$ from three readings. This brackets the estimated maximum error in Δ. This determination of the maximum negative error allows the possibility of negative values of Δ at certain flow conditions which is an unlikely if not impossible situation in reality. The implication of a negative value of Δ is that the recovery temperature is greater than the total temperature of the gas stream. For this reason, the minimum value of Δ is taken to be zero.

The error limits as given by the above expression are shown on the respective data points in Fig. 5. The random errors which have been accounted for in the error analysis contribute only a small portion to the combined error. Thus, the scatter in the data presented in Fig. 5 suggests that there are other random errors in the data which have not been considered.

SECTION V
CONCLUSIONS

The recovery temperature characteristics of a thermocouple probe of the self-aspirating type frequently used in turbine engine testing have been determined experimentally over a wide range of subsonic flow conditions. The apparatus used in this investigation circumvents the difficult

problem of direct measurement of the fluid temperature in the apparatus. The fluid temperature must be known in order to specify the thermodynamic state of the fluid and define a standard temperature with which the indicated temperature of the probe can be compared. In the apparatus, air at low velocity is heated in an indirect heat exchanger having a large amount of surface area and employing saturated steam at atmospheric pressure as an isothermal heat source. The total temperature of the fluid stream is very nearly equal to the temperature of the heat exchanger core which can be readily measured. The apparatus is well suited for calibration of probes at low gas densities corresponding, for example, to high altitude flight conditions.

In addition to providing recovery temperature correction factor data for a particular probe configuration, the results of the investigation indicate that the experimental technique is sound and can be used with confidence in calibrating other probe configurations.

A semi-empirical correlation was developed and appears to give reasonably good results over the entire range of Mach number and total pressure considered in the experimental study. The correlation permits the prediction of the effects of temperature, pressure, Mach number, and to some extent, the gas composition on temperature recovery correction.

REFERENCES

1. Hottel, H. C. and Kalitinsky, A. "Temperature Measurements in High-Velocity Air Streams." Journal of Applied Mechanics, Vol. 12, No. 1, pp. A-25 through A-32, March 1945.

2. Malmquist, Lars. "Temperature Measurements in High-Velocity Gas Streams." Transactions of the Royal Institute of Technology, Stockholm, Sweden, No. 15, 1948.

3. Stickney, T. M. "Recovery and Time-Response Characteristics of Six Thermocouple Probes in Subsonic and Supersonic Flow." NACA TN 3455, July 1955.

4. Glawe, G. E., Simmons, F. S., and Stickney, T. M. "Radiation and Recovery Corrections and Time Constants of Several Chromel-Alumel Thermocouple Probes in High-Temperature, High-Velocity Gas Streams." NACA TN 3766, October 1956.

5. Jakob, Max. Heat Transfer, Wiley, New York, 1949.

6. Sparrow, E. M. "Analysis of Laminar Forced-Convection Heat Transfer in Entrance Region of Flat Rectangular Ducts." NACA TN 3331, January 1955.

7. Schneider, Paul J. Conduction Heat Transfer, Addison-Wesley Publishing Company, Cambridge, Massachusetts, 1955.

APPENDIXES

I. ILLUSTRATIONS
II. TABLES
III. AN ANALYSIS TO DETERMINE HEAT EXCHANGER EFFECTIVENESS
IV. AN ANALYSIS OF A SELF-ASPIRATING THERMOCOUPLE PROBE

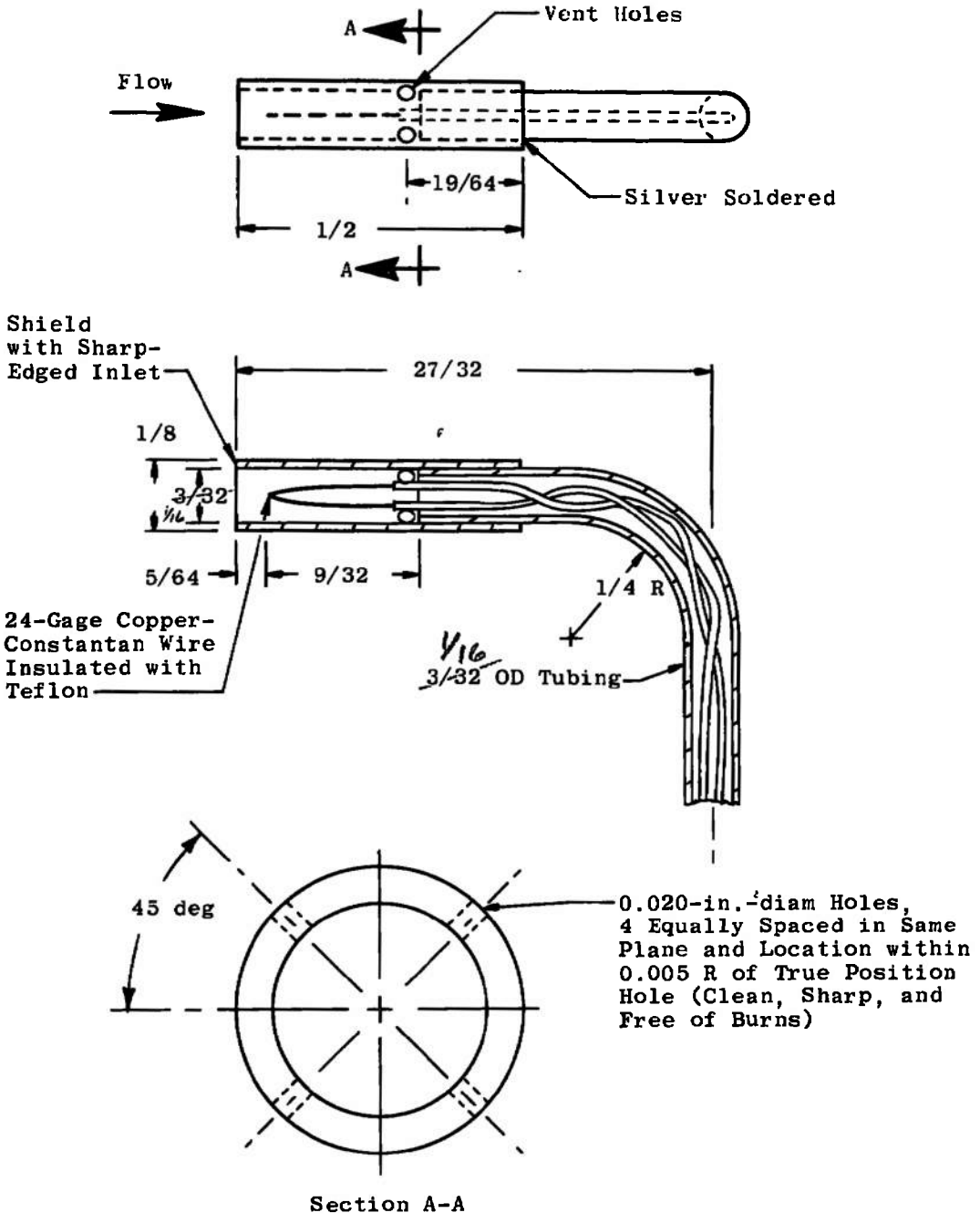

Notes: Dimensions, wire size, and wire type are the same as in General Electric Drawing No. 4012303-610.

All dimensions are in inches.

a. Schematic of Self-Aspirating Thermocouple Probe Tested in the Present Study

Fig. 1 Thermocouple Probes

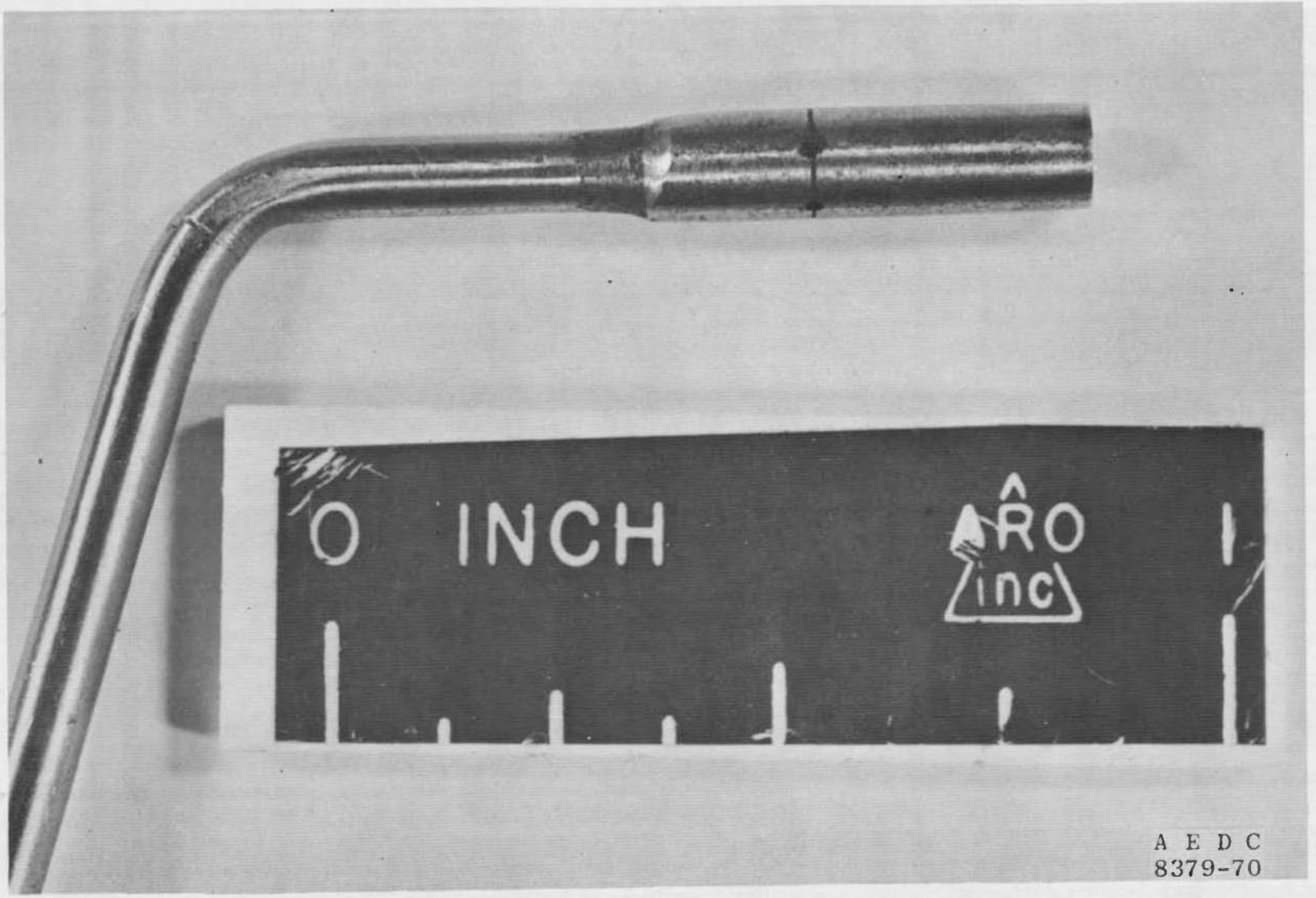

b. Photograph of Self-Aspirating Thermocouple Probe Tested in the Present Study

Fig. 1 Continued

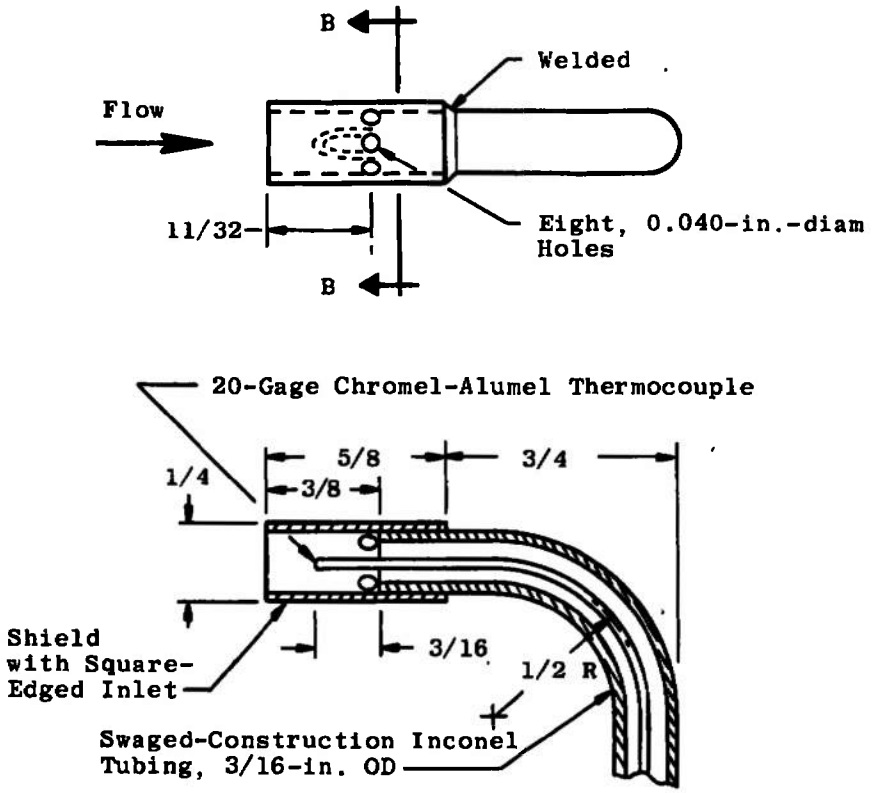

c. Schematic of Self-Aspirating Thermocouple Probe Tested by Glawe, Simmons, and Stickney (Ref. 4)
Fig. 1 Concluded

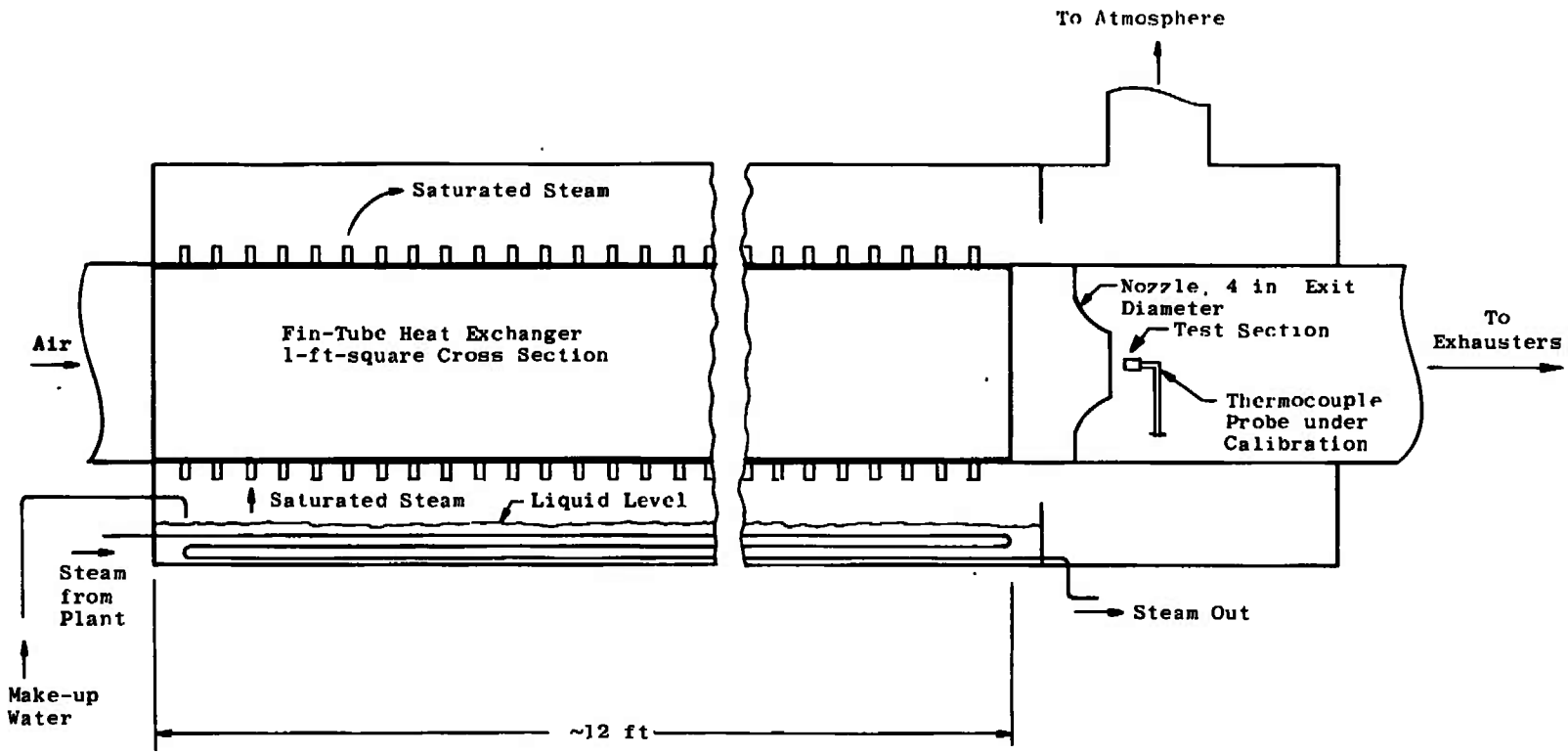

a. Heat Exchanger and Steam Generator

Fig. 2 Schmatics of Experimental Apparatus

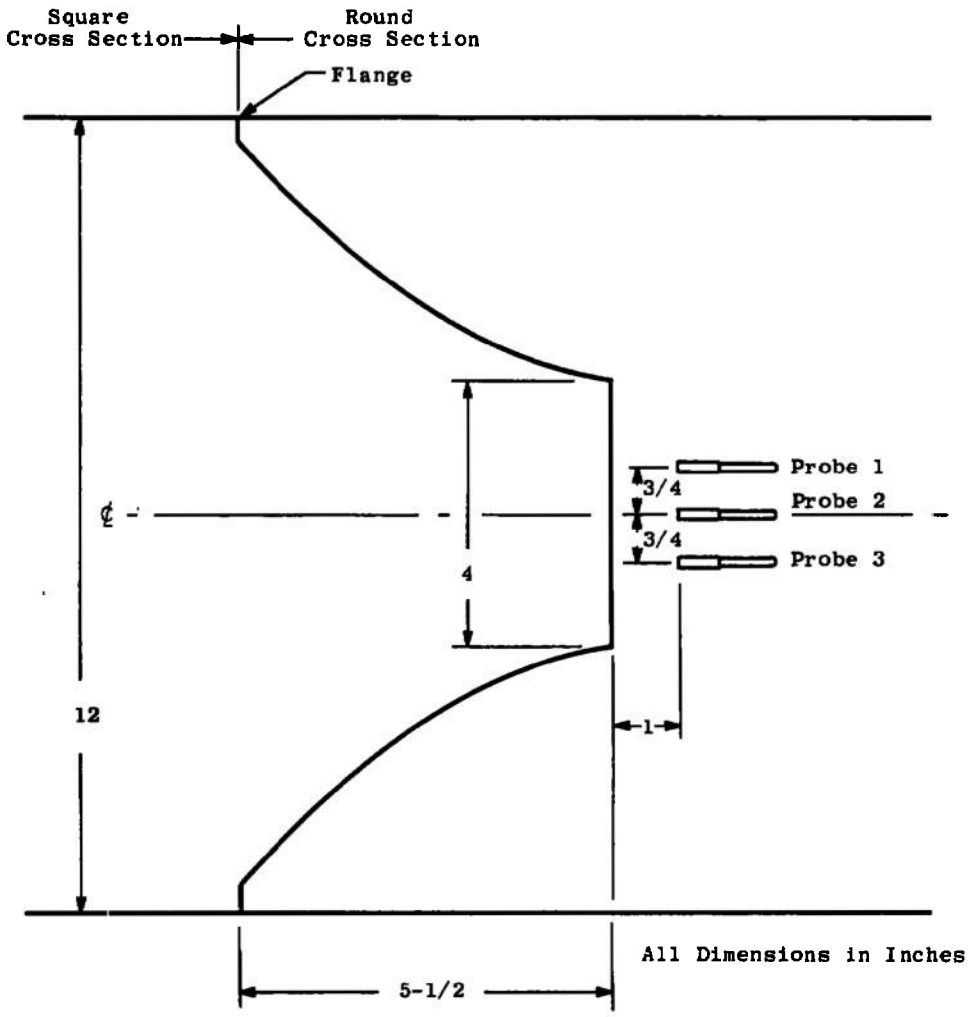

b. Detail of Nozzle and Test Section
Fig. 2 Concluded

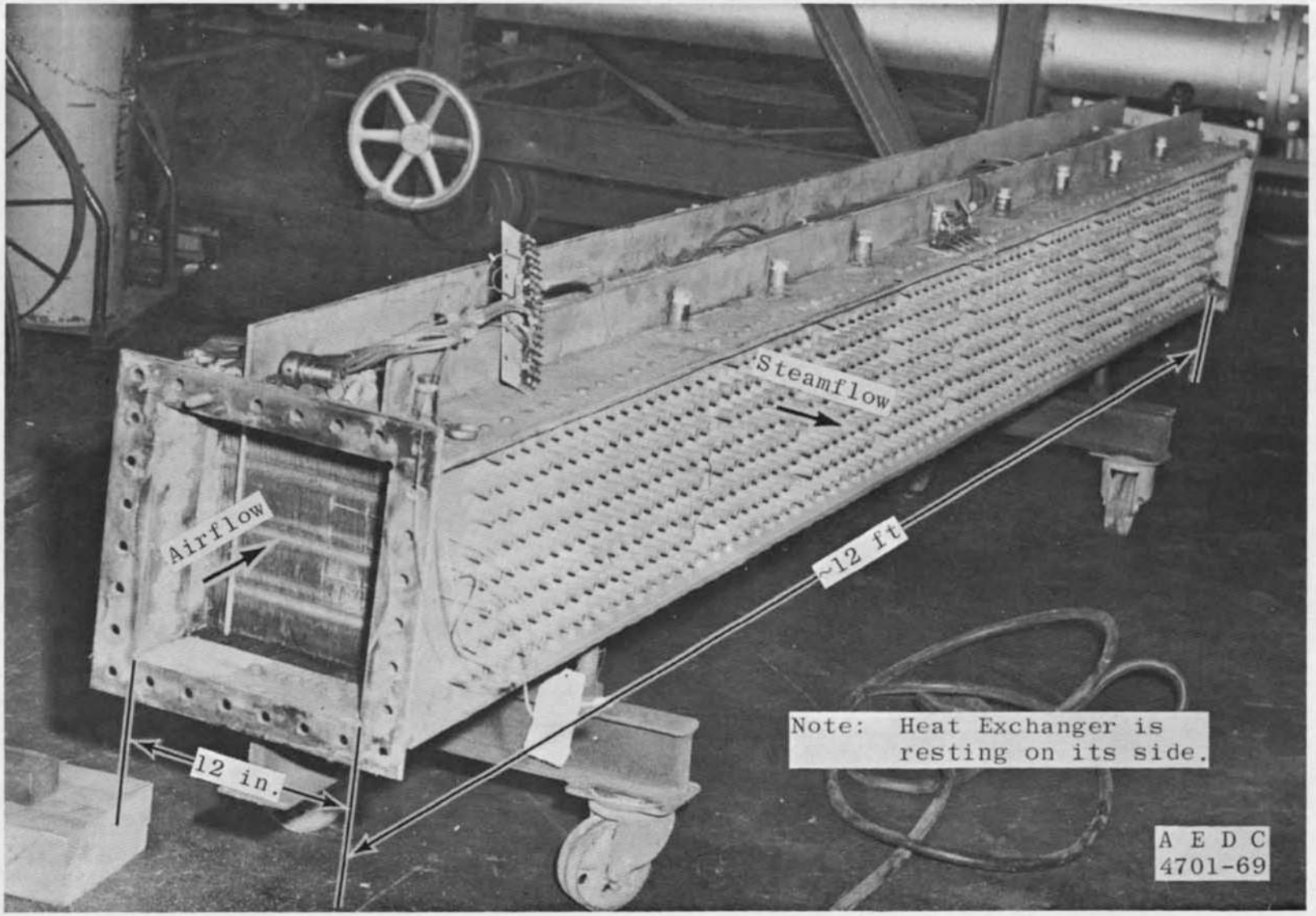

Fig. 3 Photograph of Heat Exchanger

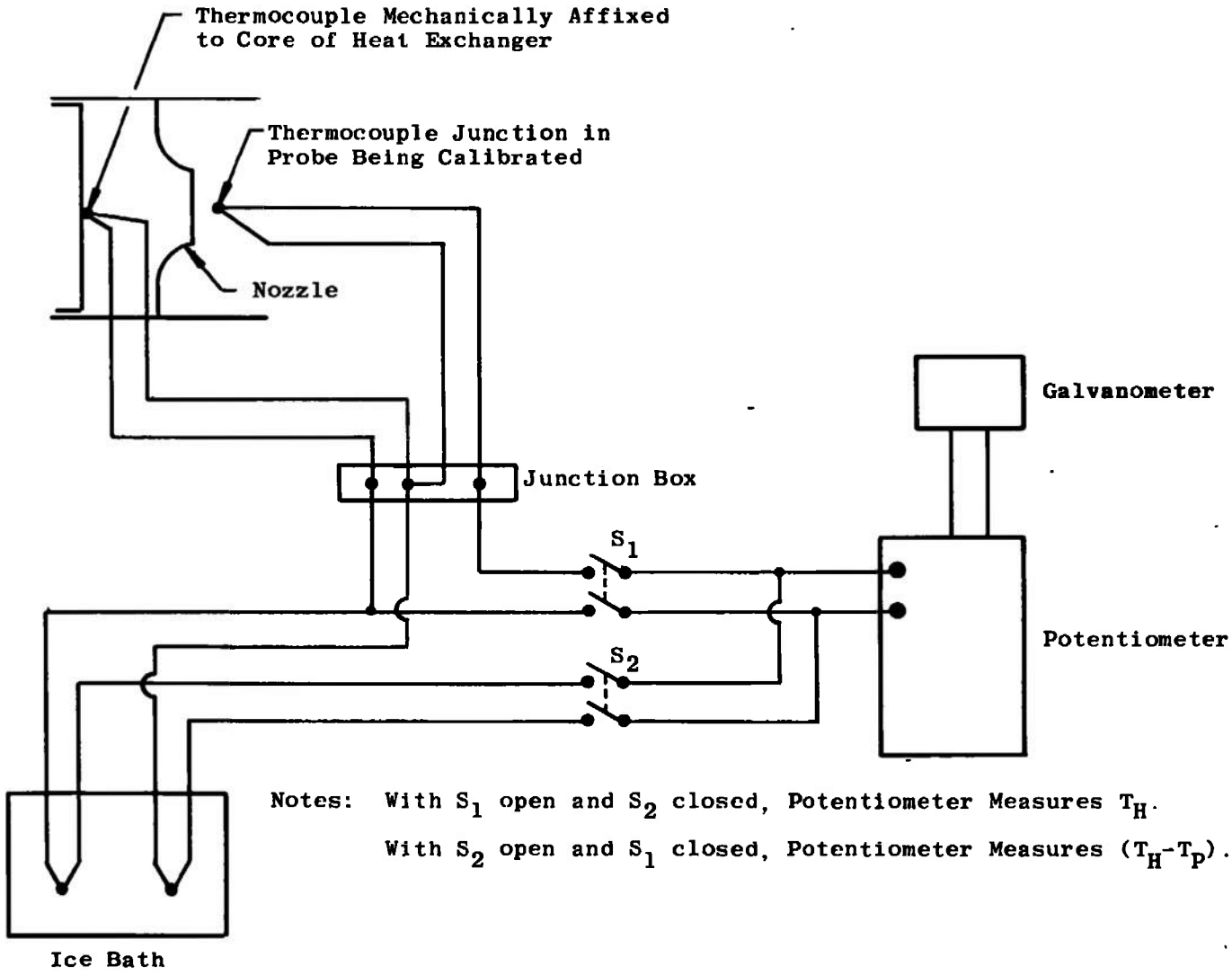

Fig. 4 Schematic Diagram of Thermocouple Circuitry

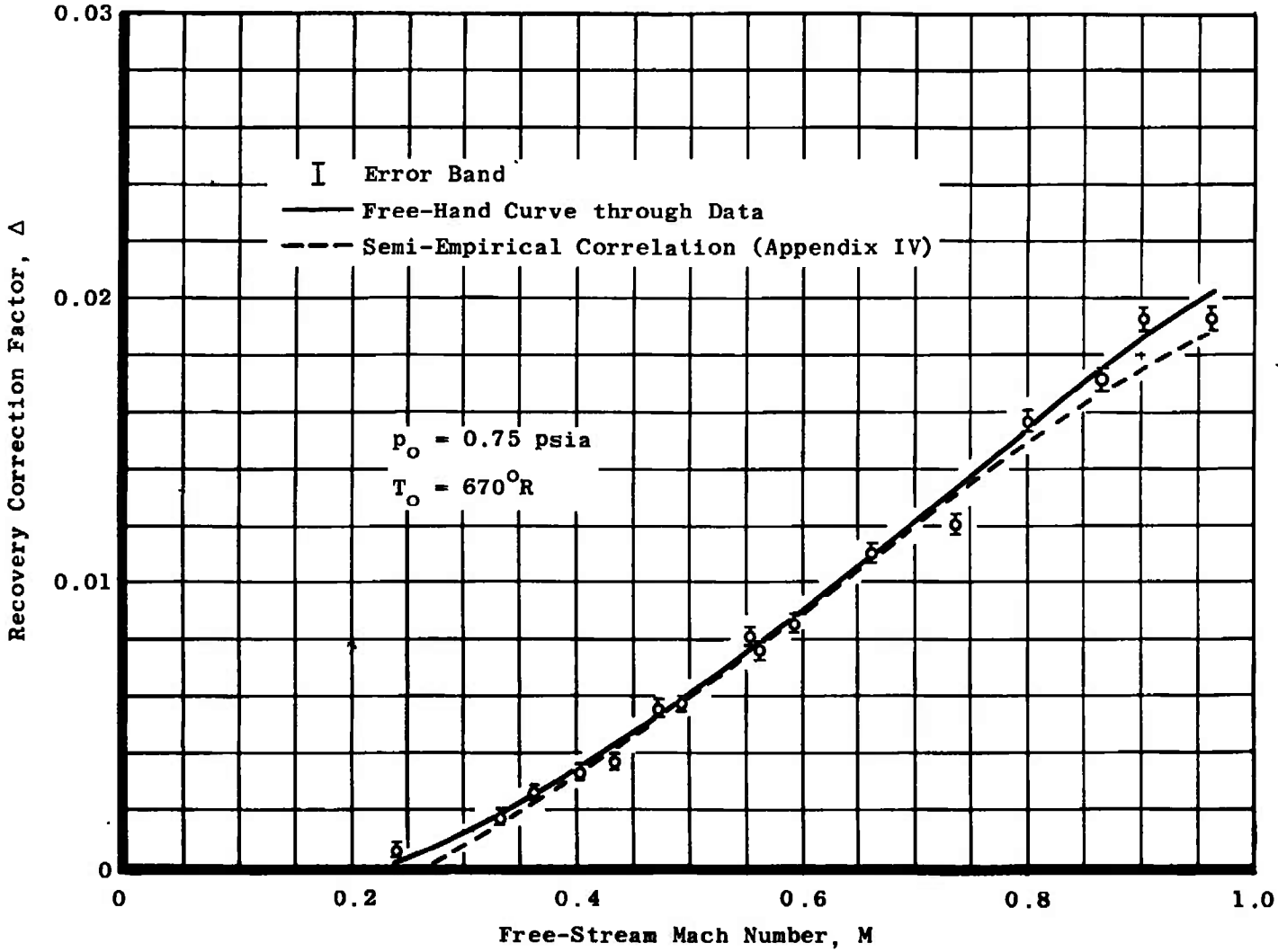

a. Total Pressure 0.75 psia

Fig. 5 Variation in Average Recovery Correction Factor with Mach Number and Total Pressure

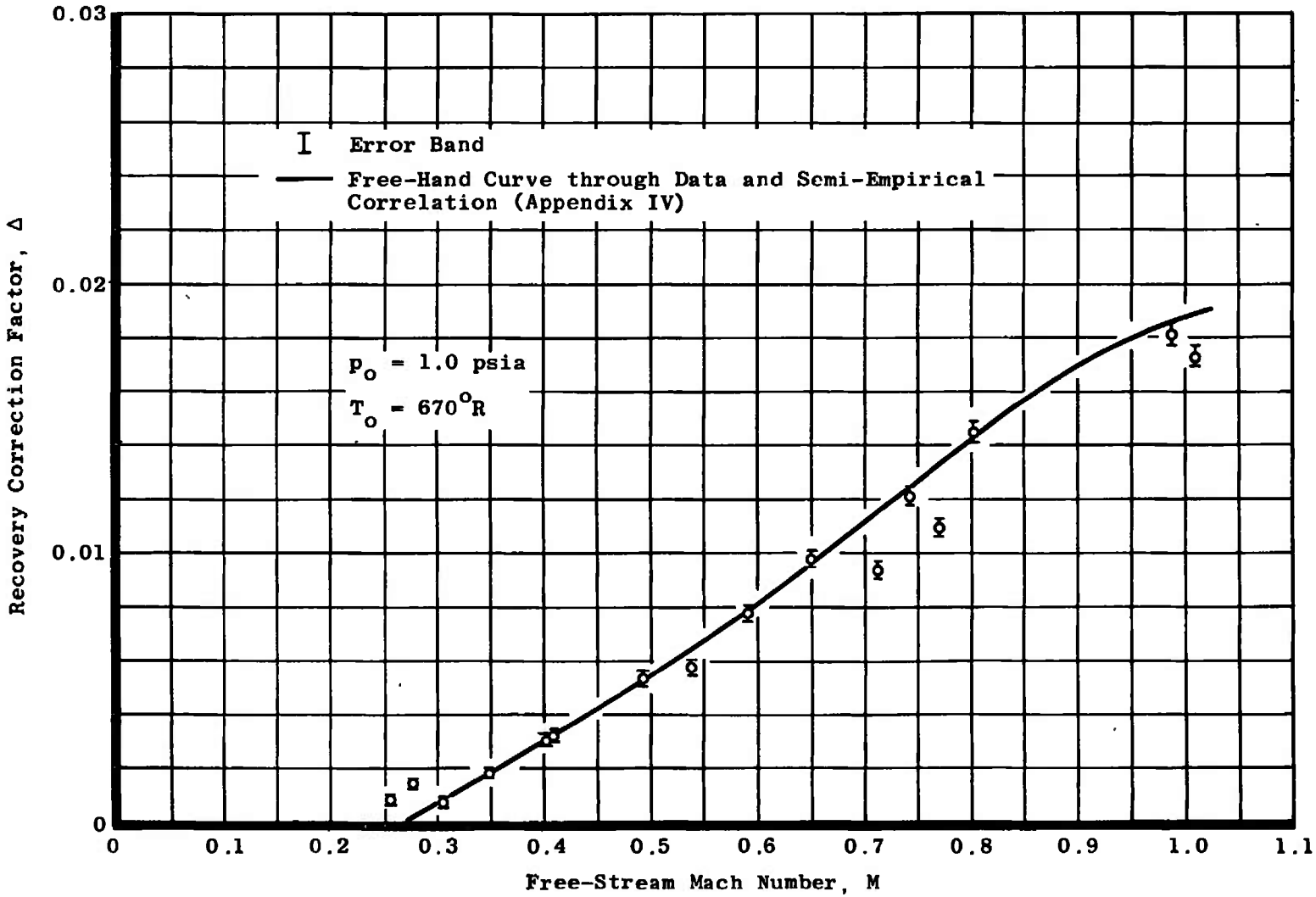

b. Total Pressure 1.0 psia
Fig. 5 Continued

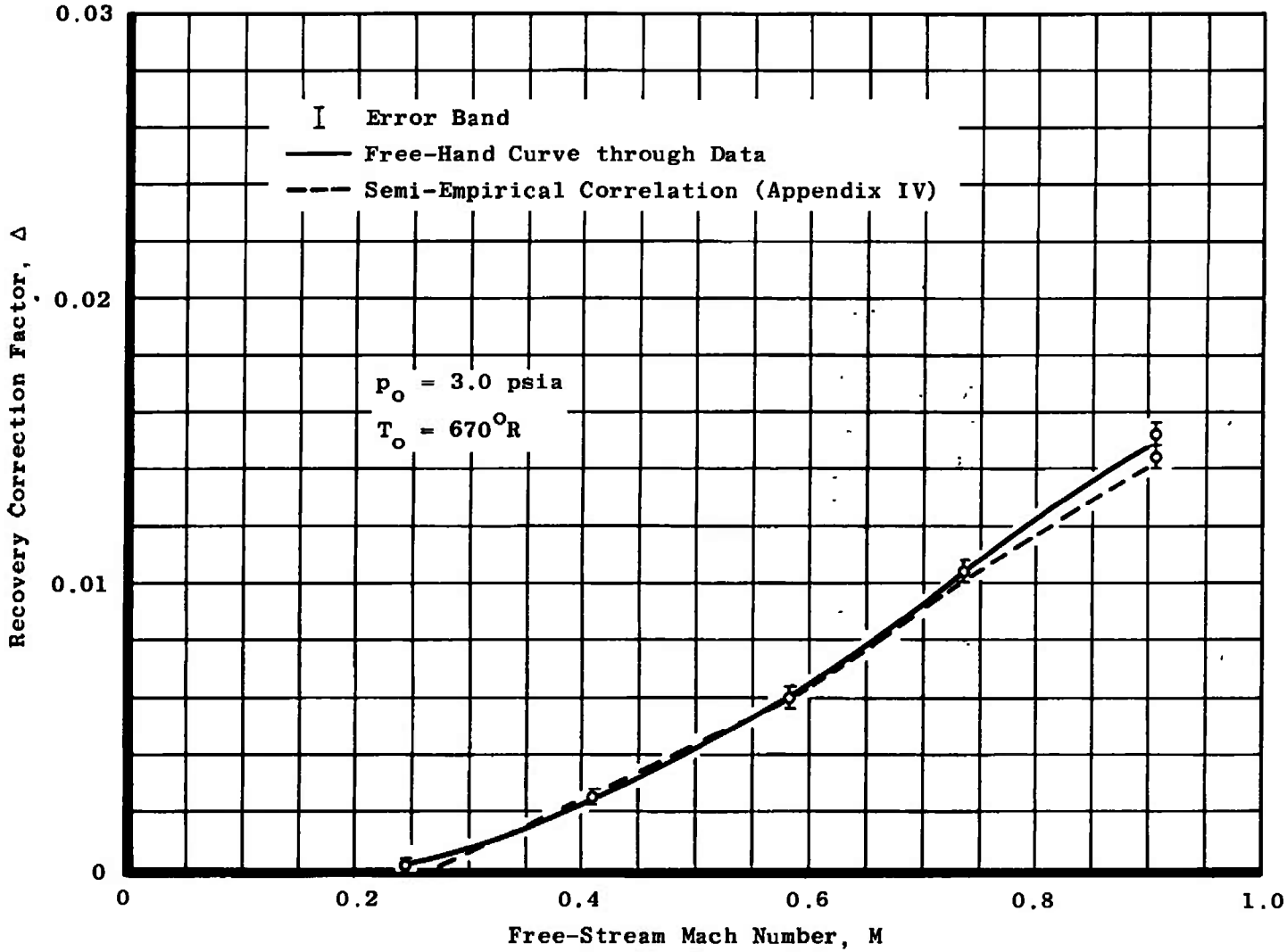

c. Total Pressure 3.0 psia
Fig. 5 Continued

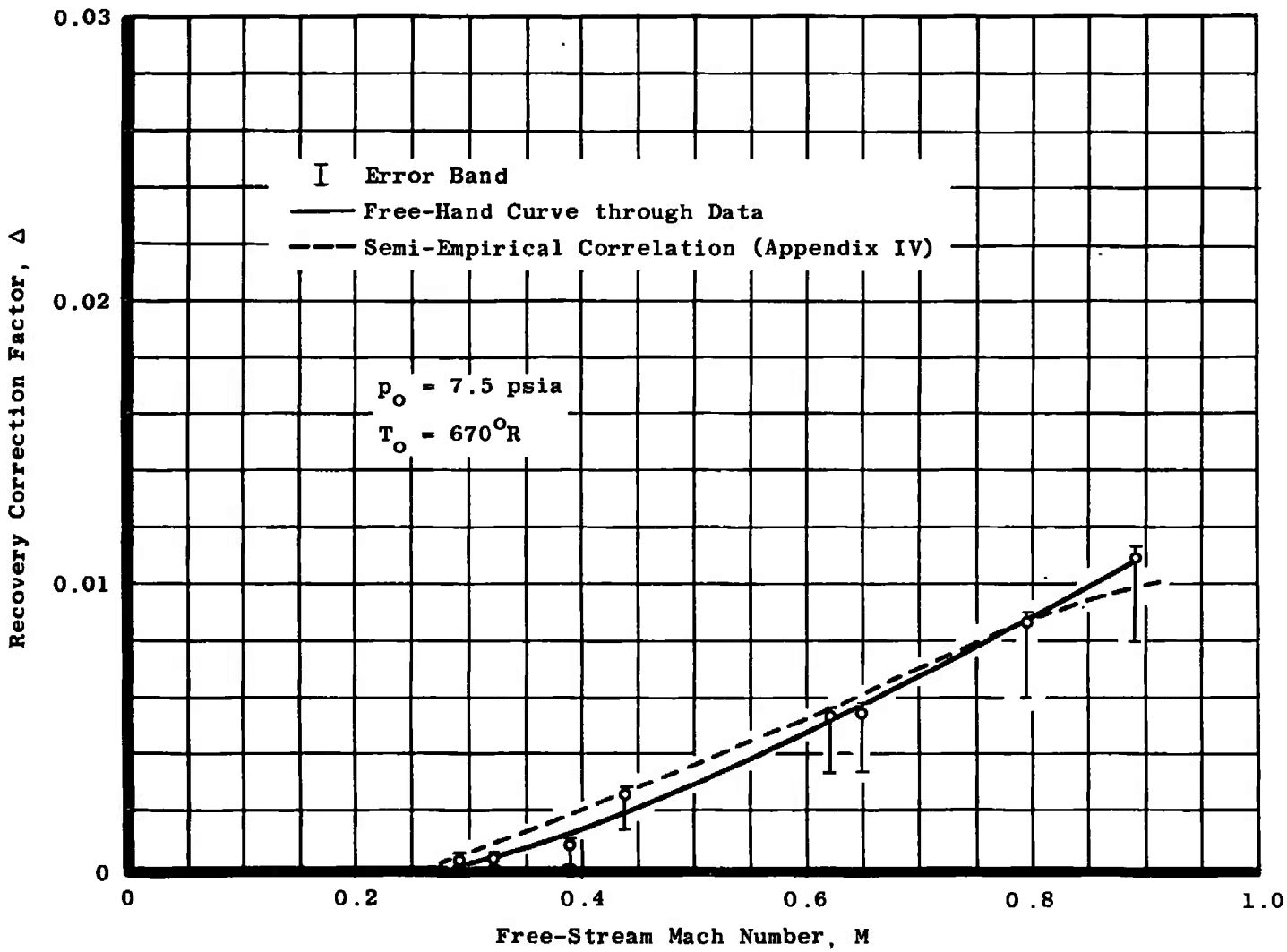

d. Total Pressure 7.5 psia
Fig. 5 Continued

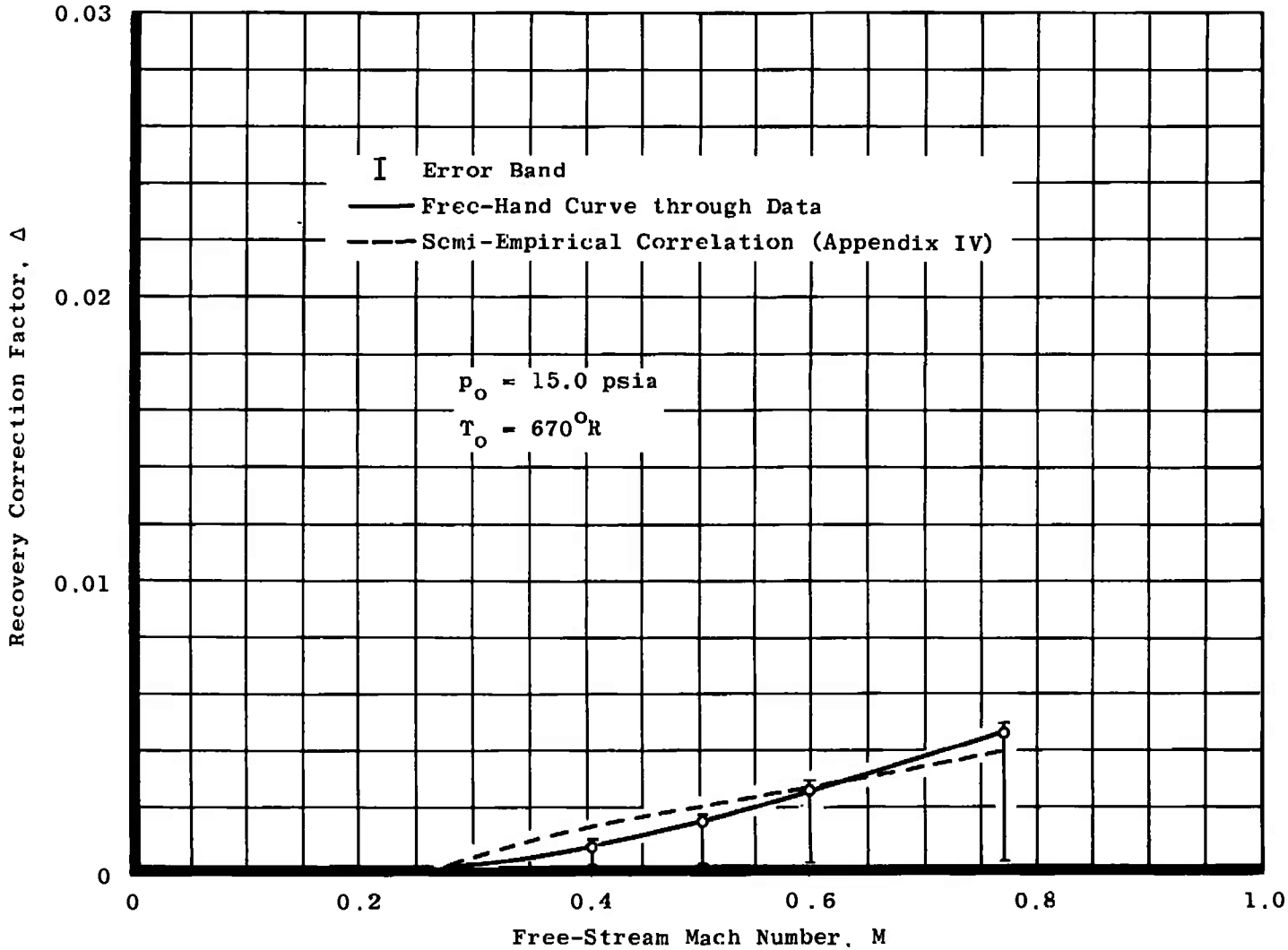

e. Total Pressure 15.0 psia
Fig. 5 Concluded

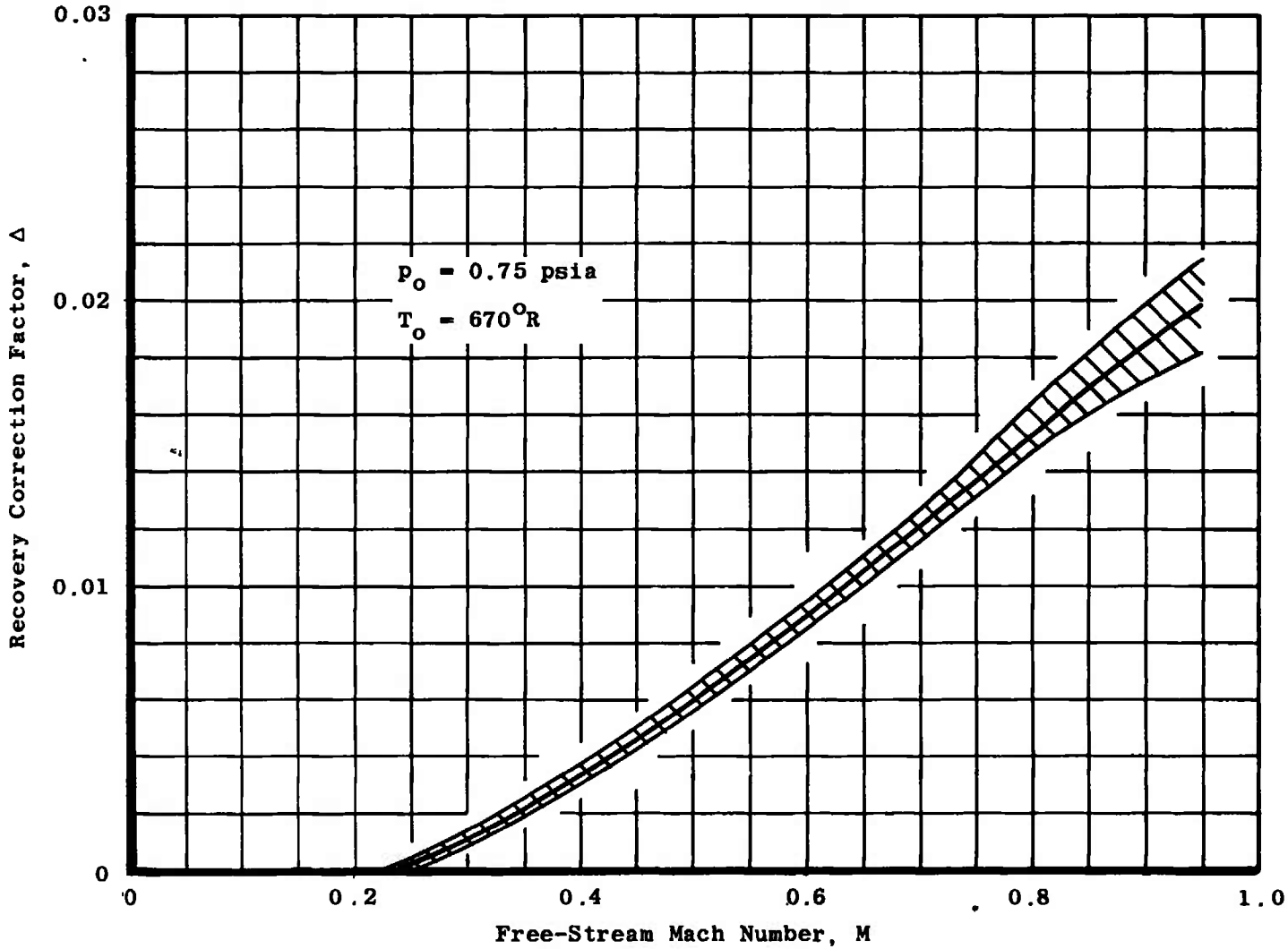

a. Total Pressure 0.75 psia

Fig. 6 Smoothed Recovery Factor Data versus Mach Number and Total Pressure

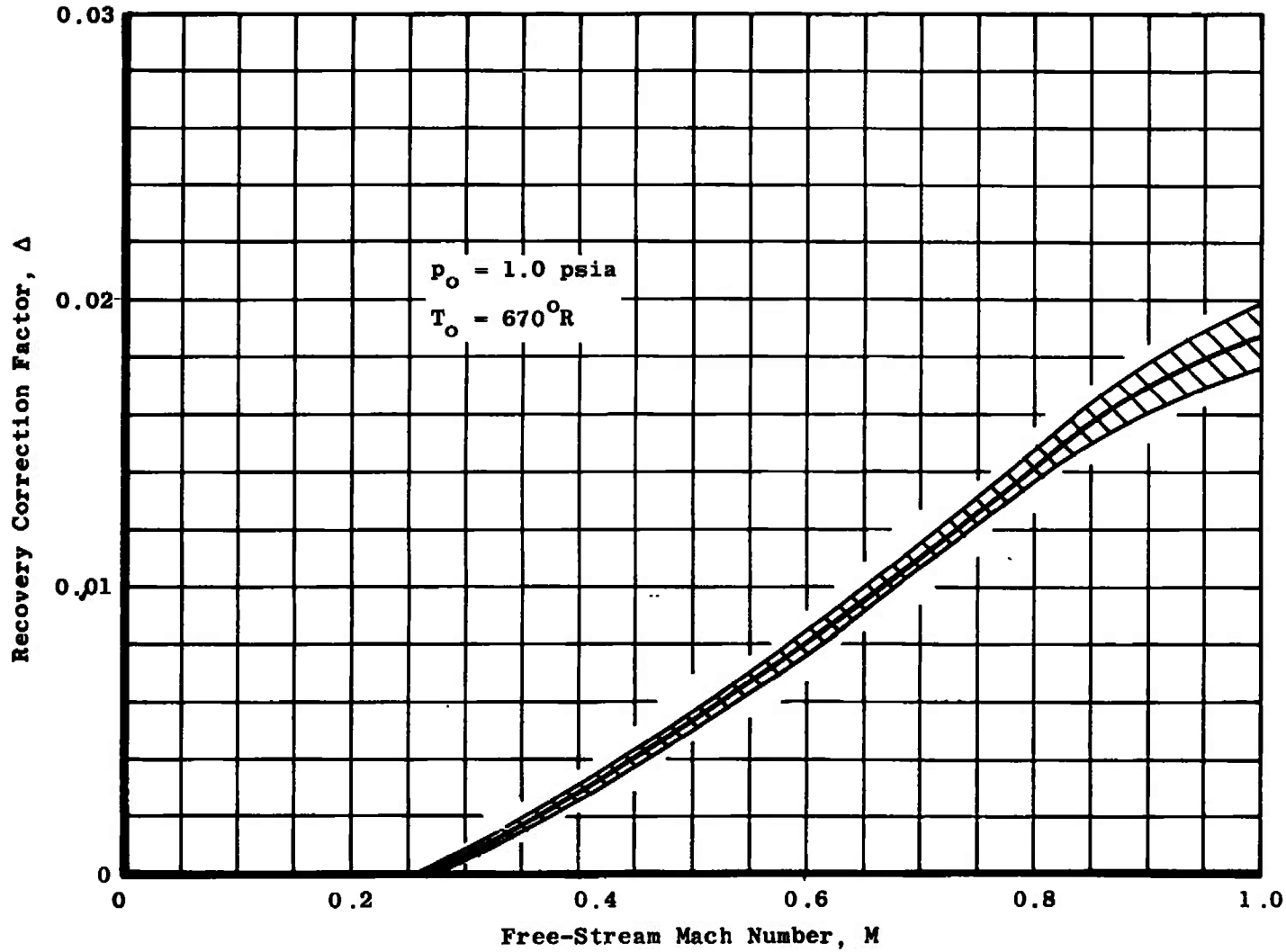

b. Total Pressure 1.0 psia
Fig. 6 Continued

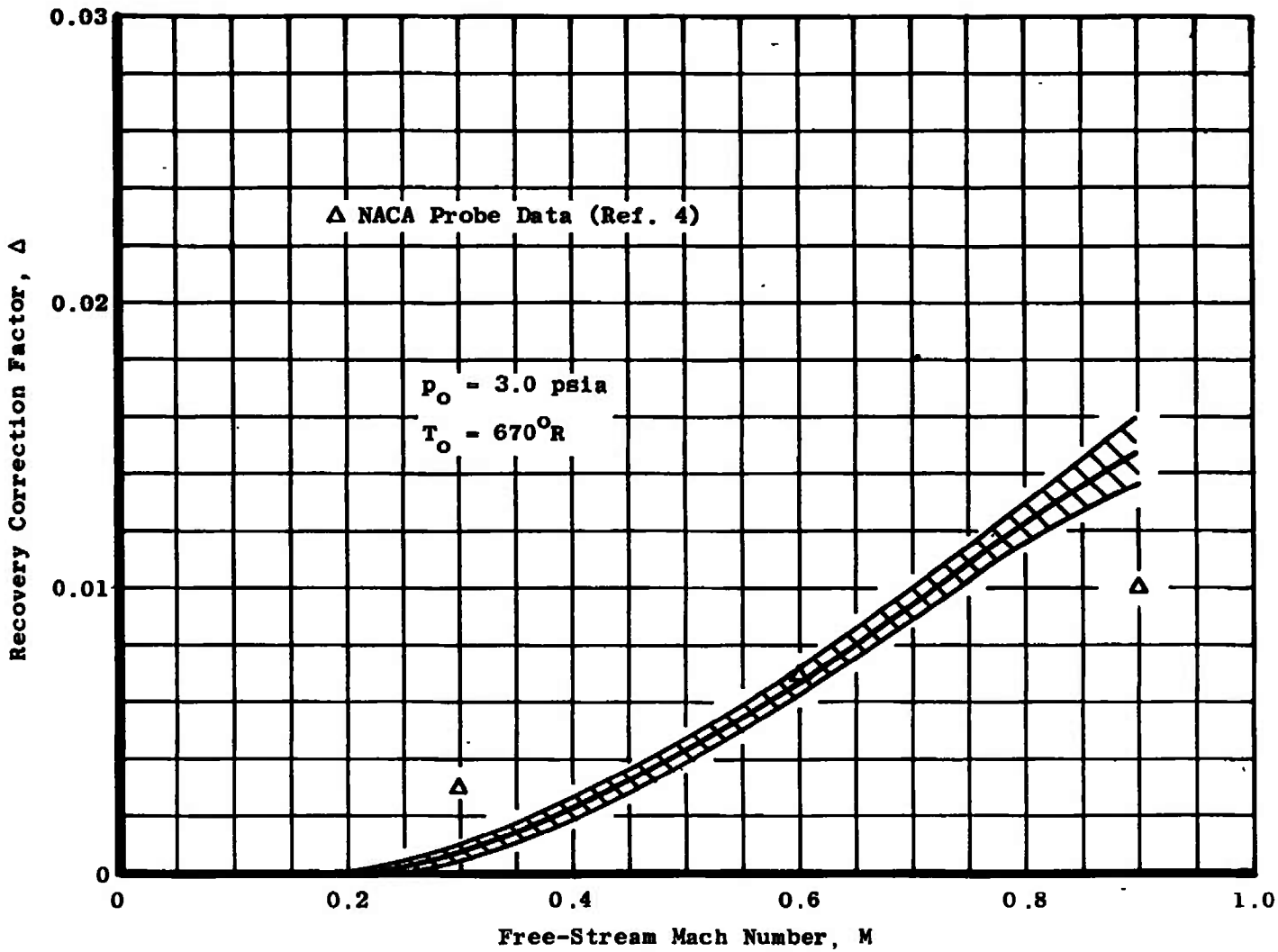

c. Total Pressure 3.0 psia
Fig. 6 Continued

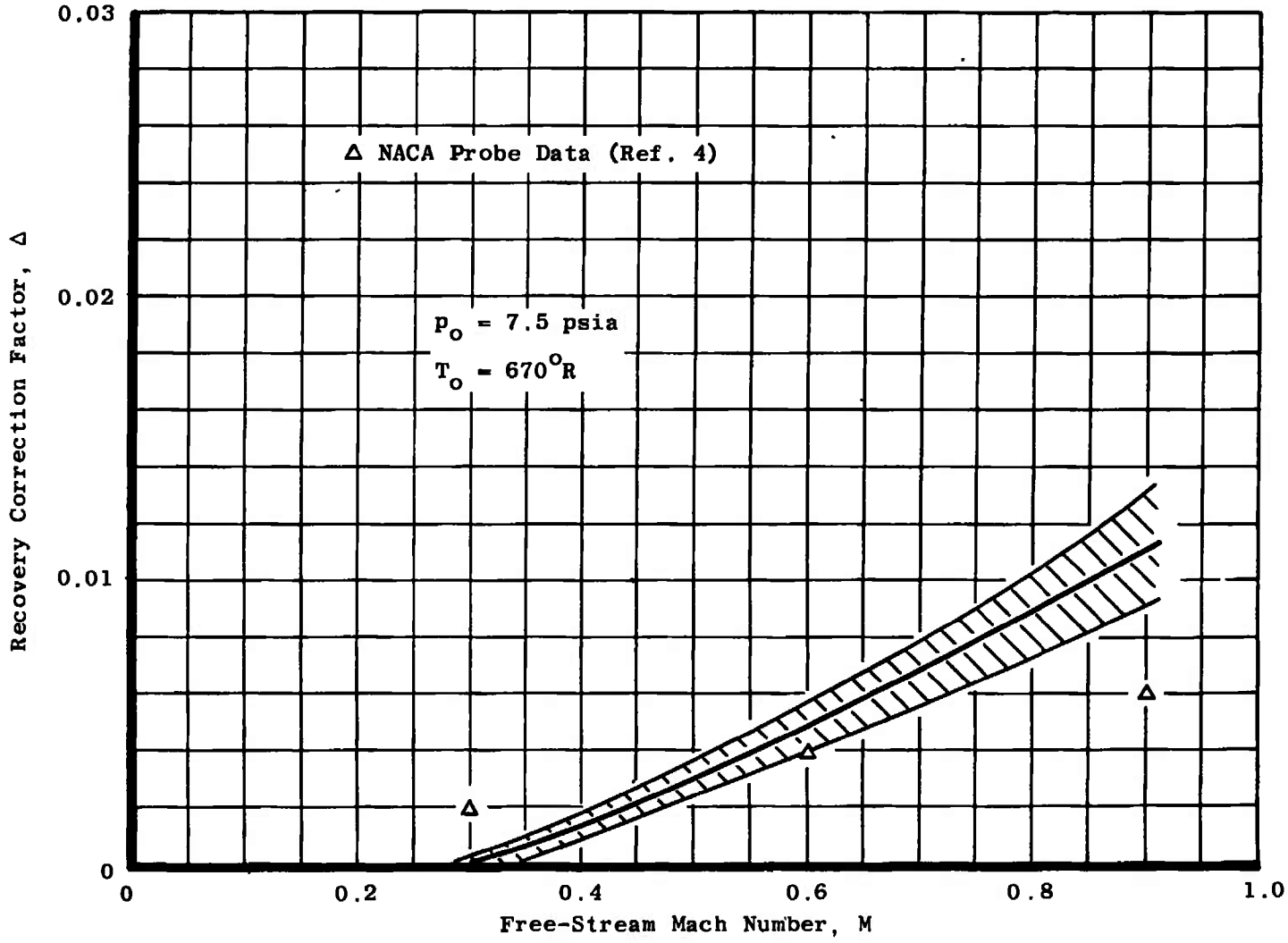

d. Total Pressure 7.5 psia
Fig. 6 Continued

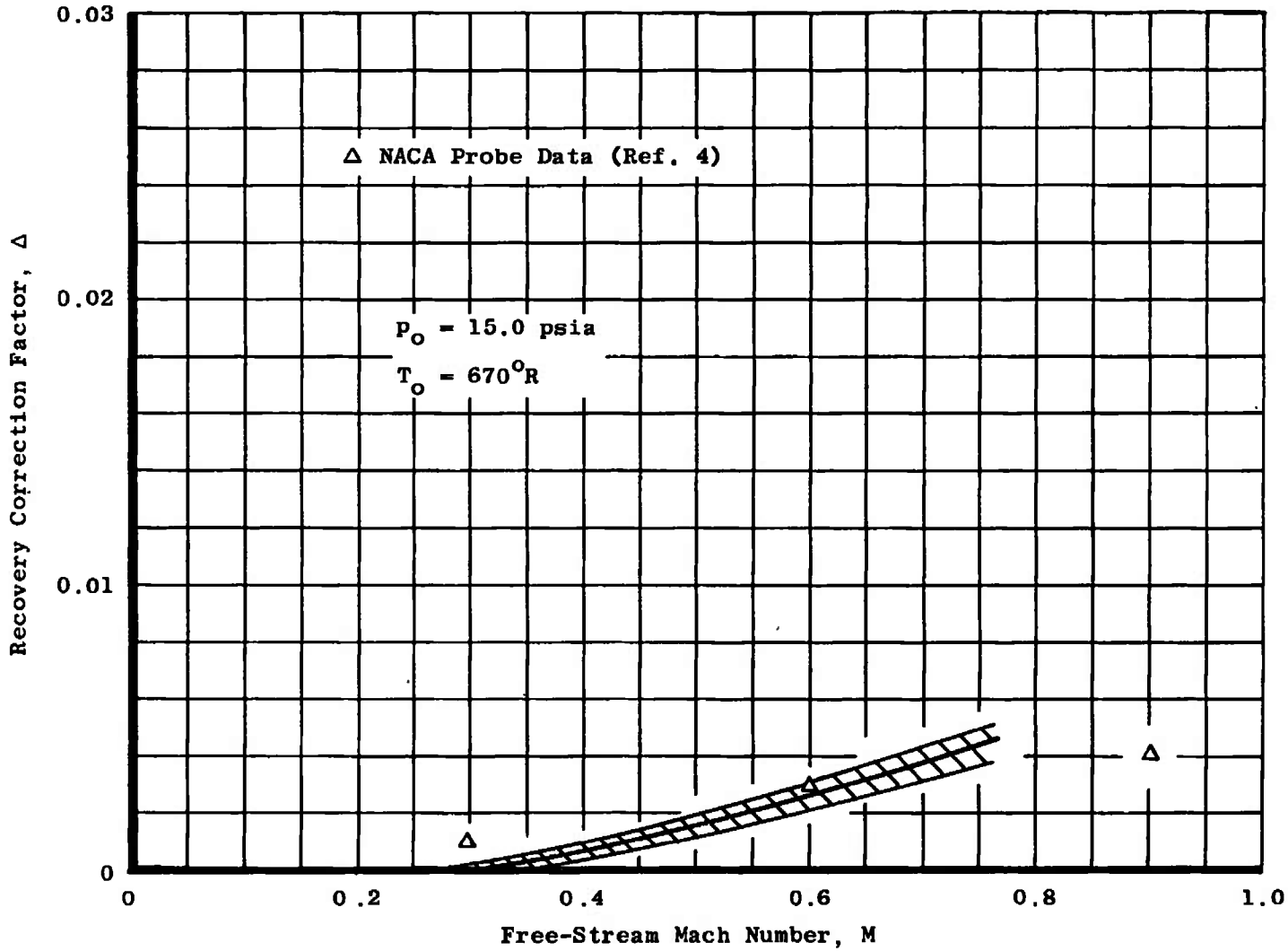

e. Total Pressure 15.0 psia
Fig. 6 Concluded

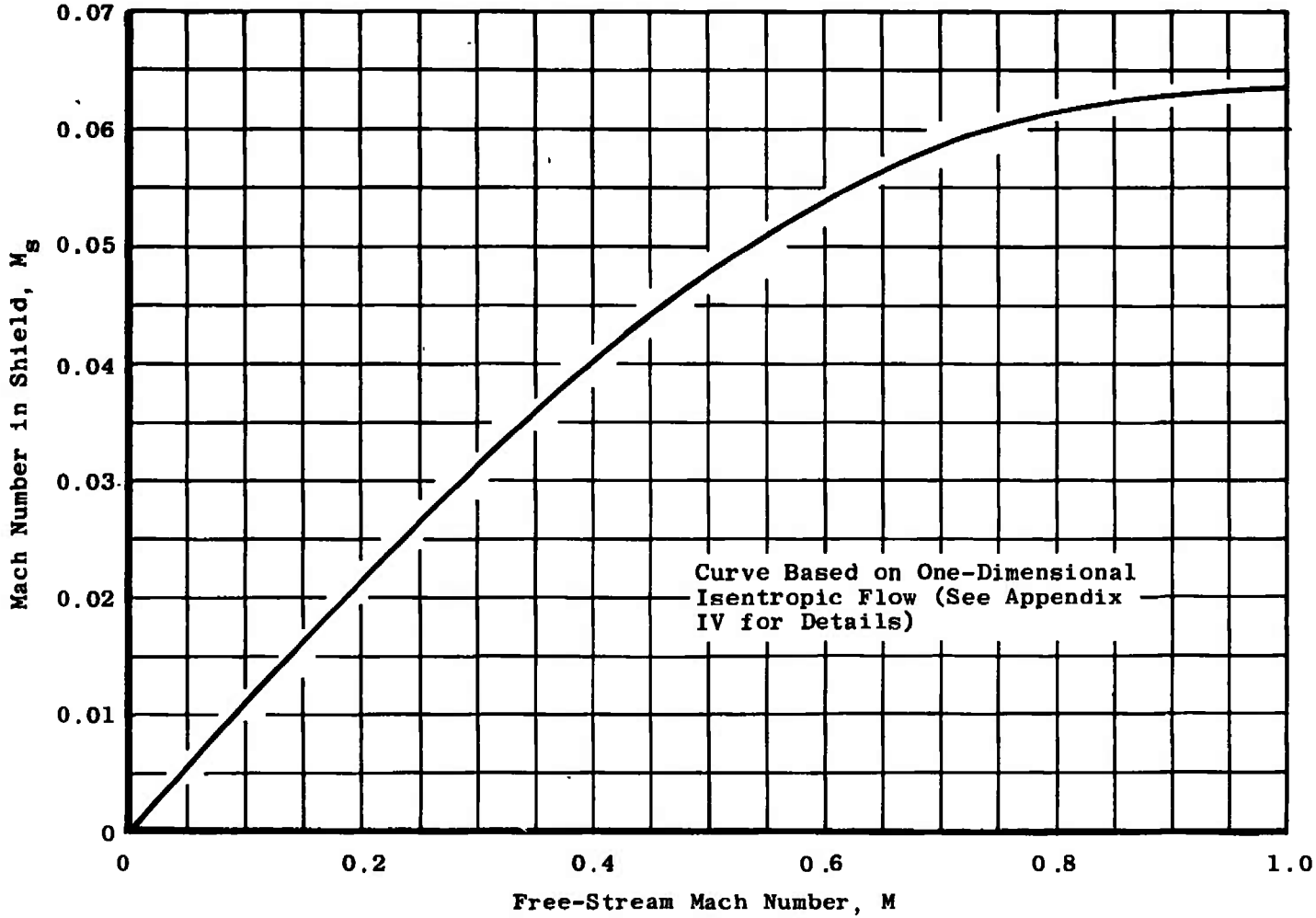

Fig. 7 Mach Number of Flow inside Shield of Probe Shown in Fig. 1a

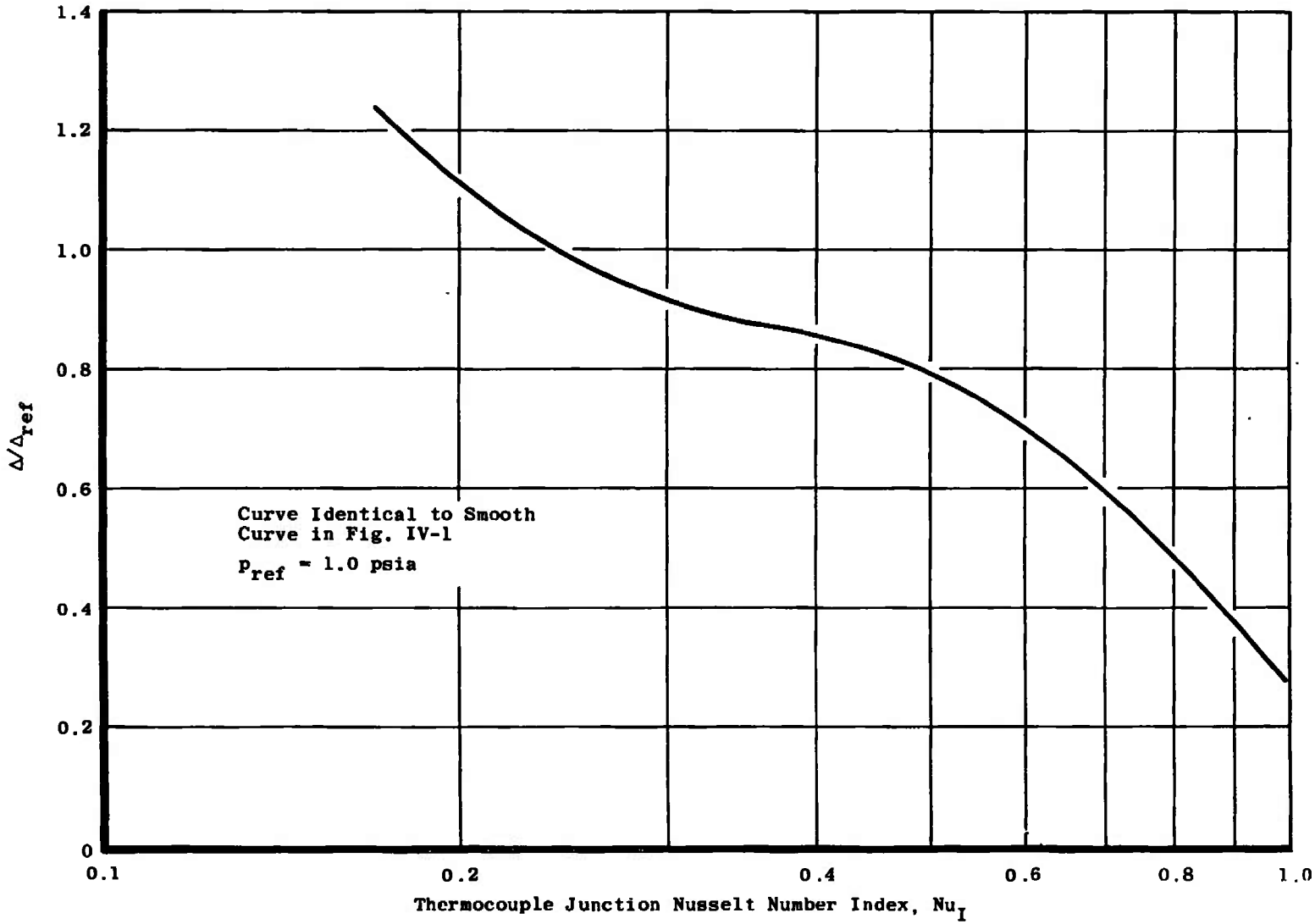

Fig. 8 Recovery Correction Factor Ratio versus Nusselt Number Index

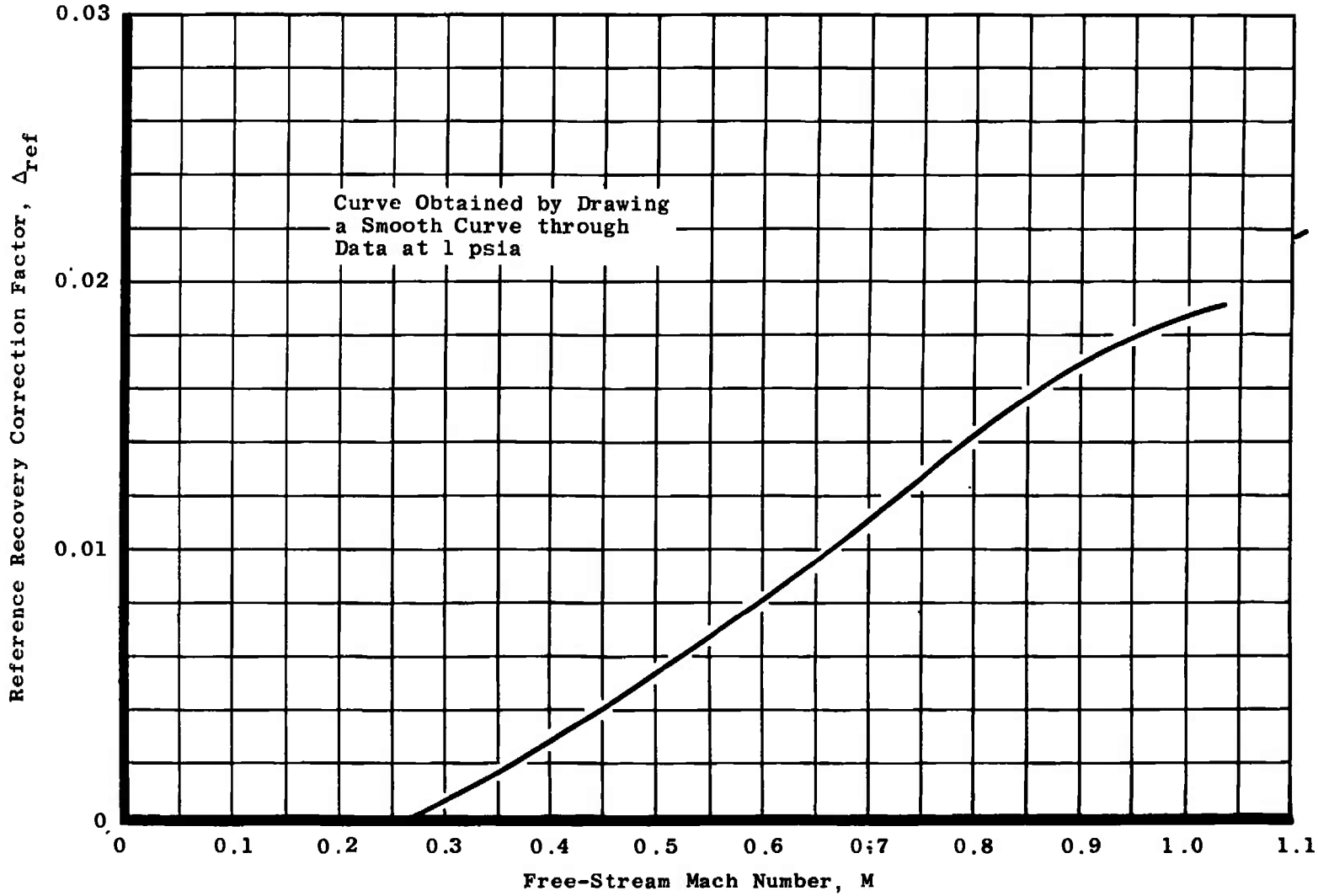

Fig. 9 Reference Recovery Correction versus Mach Number

TABLE I
THERMOCOUPLE PROBE RECOVERY CORRECTION FACTOR DATA

a. Total Pressure 0.75 psia

Mach Number, M	Total Pressure, p_o psia	Recovery Correction Factor			
		Probe 1	Probe 2	Probe 3	Average
0.237	0.750	0.00049	0.00045	0.00074	0.000561
0.328	0.753	0.00157	0.00178	0.00164	0.00166
0.361	0.753	0.00218	0.00269	0.00290	0.00259
0.402	0.750	0.00315	0.00363	0.00322	0.00333
0.431	0.750	0.00340	0.00391	0.00360	0.00363
0.472	0.738	0.00515	0.00576	0.00576	0.00556
0.492	0.754	0.00467	0.00618	0.00618	0.00568
0.553	0.751	0.00736	0.00836	0.00836	0.00803
0.561	0.750	0.00709	0.0080	0.00779	0.00763
0.591	0.735	0.00808	0.00882	0.00876	0.00855
0.660	0.753	0.01027	0.01153	0.01112	0.01097
0.735	0.753	0.01309	0.01476	0.01399	0.01395
0.736	0.749	0.01347	0.01467	0.01351	0.01388
0.800	0.732	0.01524	0.01572	0.01593	0.0156
0.866	0.754	0.01558	0.01834	0.01709	0.0170
0.900	0.748	0.01769	0.02070	0.01904	0.01914
0.959	0.754	0.01785	0.02079	0.01864	0.01910

Note: Total Temperature is 670°R.

b. Total Pressure 1.0 psia

Mach Number, M	Total Pressure, p_o psia	Recovery Correction Factor			
		Probe 1	Probe 2	Probe 3	Average
0.254	1.057	0.000626	0.000955	0.0009701	0.00085
0.277	0.970	0.000955	0.00149	0.00173	0.001393
0.305	0.977	0.000597	0.000896	0.000746	0.000746
0.348	0.985	0.001657	0.00191	0.00194	0.00184
0.403	1.02	0.00228	0.00333	0.00333	0.00298
0.407	0.986	0.00279	0.00327	0.00327	0.00312
0.493	0.995	0.00518	0.00525	0.00548	0.0053
0.537	1.01	0.00490	0.00603	0.00603	0.00565
0.591	0.992	0.00755	0.00766	0.00788	0.0077
0.650	1.004	0.00937	0.00996	0.00973	0.00969
0.713	1.00	0.00825	0.00975	0.00966	0.00922
0.743	1.01	0.01164	0.01222	0.01203	0.01196
0.770	1.01	0.00991	0.01134	0.00111	0.01080
0.8036	0.998	0.0139	0.0149	0.0145	0.0144
0.987	1.01	0.01679	0.01896	0.0183	0.01802
1.01	1.01	0.01597	0.01788	0.01772	0.0172

Note: Total Temperature is 670°R.

TABLE I (Concluded)

c. Total Pressure 3.0 psia

Mach Number, M	Total Pressure, p_o psia	Recovery Correction Factor			
		Probe 1	Probe 2	Probe 3	Average
0.241	3.02	0.000119	0.000239	0.000269	0.000209
0.407	3.00	0.00228	0.00260	0.00260	0.00249
0.581	2.997	0.00548	0.00625	0.00603	0.00592
0.734	2.980	0.00970	0.01110	0.01030	0.0104
0.903	3.00	0.01306	0.01572	0.01443	0.0144
0.904	3.00	0.01439	0.01646	0.01482	0.0152

Note: Total Temperature is 670°R.

d. Total Pressure 7.5 psia

Mach Number, M	Total Pressure, p_o psia	Recovery Correction Factor			
		Probe 1	Probe 2	Probe 3	Average
0.248	7.48	---	---	---	---
0.292	7.54	0.00025	0.00037	0.00045	0.000358
0.320	7.50	0.00051	0.00045	0.000037	0.000185
0.390	7.497	0.000134	0.00149	0.00085	0.000826
0.440	7.507	0.002104	0.002940	0.002746	0.00260
0.621	7.49	0.00452	0.00581	0.00588	0.00540
0.649	7.49	0.00445	0.00633	0.00576	0.00551
0.796	7.50	0.00734	0.00975	0.00891	0.00867
0.893	7.50	0.00885	0.01264	0.01148	0.01099

Note: Total Temperature is 670°R.

e. Total Pressure 15.0 psia

Mach Number, M	Total Pressure, p_o psia	Recovery Correction Factor			
		Probe 1	Probe 2	Probe 3	Average
0.403	15.0	0.000858	0.000896	0.00045	0.000715
0.503	15.0	0.00119	0.00196	0.00142	0.00152
0.597	15.0	0.00218	0.00309	0.00248	0.00258
0.770	15.0	0.00399	0.00491	0.00476	0.00455

Note: Total Temperature is 670°R.

APPENDIX III
AN ANALYSIS TO DETERMINE HEAT EXCHANGER EFFECTIVENESS

The purpose of this appendix is to obtain an estimate of the difference between the air leaving the heat exchanger and the steam temperature.

Figure 3 shows a photograph of the fin-tube heat exchanger used in the apparatus to heat the air to a known temperature. The heat exchanger has an effective length of approximately 11 ft and a 1-ft-square cross section. The aluminum fins are 0.0125 in. thick, and there are approximately 110 fins per foot. The brass tubes have an outside diameter of 5/8 in. with a 1/32-in. wall thickness and are arranged in equilateral, staggered triangles on 1-1/2-in. centers.

The rate of heat transfer to the air from the steam for a differential length of heat exchanger (dx) is

$$d\dot{Q} = (U_F W_F + U_T W_T)(T_s - T_b)\, dx \qquad \text{(III-1)}$$

where U_F and U_T are the overall heat transfer coefficients for the fins and tubes, respectively, and W_F and W_T are surface areas per unit length consistent with the definitions of U_F and U_T. Conservation of energy requires

$$d\dot{Q} = G C_p\, d T_b \qquad \text{(III-2)}$$

Since saturated steam at constant pressure is used as the heat source, the steam temperature T_S is constant. If it is assumed that U_F, U_T, and C_p are constant, Eq. (III-2) can be integrated to give

$$\ln \frac{T_{b_2} - T_s}{T_{b_1} - T_s} = - \frac{(U_F W_F + U_T W_T) L}{G C_p} \qquad \text{(III-3)}$$

where T_{b2} and T_{b1} are inlet and exit air temperatures, respectively, and L is the total heat exchanger length.

The heat transfer coefficients U_F and U_T must be evaluated through consideration of airflow in the heat exchanger, condensation of steam inside the tubes, and heat conduction through the fins and tubes. It can be shown that

$$U_T = \frac{1}{\frac{1}{h_T} + \frac{D_o \ln D_o/D_i}{2 k_T} + \frac{D_o}{h_S D_i}} \qquad \text{(III-4)}$$

where h_T is a suitable heat transfer coefficient for flow over a finned tube and h_S is the heat transfer on the steam side of the tubes. The surface area W_T is the total surface area of the tubes alone exposed to the airflow per unit length of heat exchanger. The heat transfer coefficient for the fins can be shown to be

$$U_F = \frac{1}{\frac{1}{\eta_F h_F} + \frac{A_F \ell n\, D_o/D_i}{2\pi k_T t} + \frac{A_F}{\pi D_i t h_S}} \qquad \text{(III-5)}$$

where A_F is the surface area of fin exposed to the air per tube and per fin. For this case, the surface area W_F is the total fin area per unit length of heat exchanger exposed to the airflow.

In order to proceed further with the analysis, it is necessary to have estimates of the heat transfer coefficients h_S, h_F, and h_T as well as the fin efficiency η_F.

From data on condensation of saturated steam in a vertical tube presented in Ref. 5, it can be inferred that

$$h_S = 674 \sqrt[3]{\frac{3.98}{H}} \text{ ft, } \frac{\text{Btu}}{\text{ft}^2\text{-hr-}^\circ\text{R}} \qquad \text{(III-6)}$$

when the vapor velocity in the tube is low. In this formula, H is the cooled height of the tube which is one foot for the heat exchanger under consideration. Thus,

$$h_S = 1065 \text{ Btu/ft}^2\text{-hr-}^\circ\text{R}$$

In cross section along the direction of airflow, the fins in the heat exchanger have a wavy surface to promote turbulence in the flow for effective heat exchange. However, for purposes of analysis, the fins will be taken to be flat and flow between any two adjacent fins will be treated as laminar and fully developed channel flow. Clearly, this will yield a conservative estimate of h_F. For fully developed laminar flow in a channel, Ref. 6 gives

$$\frac{2 h_F (S - t)}{k_a} = 7.5$$

Since the thermal conductivity of air k_a does not change markedly over the temperature range of interest

$$h_F = 7.9 \text{ Btu/ft}^2\text{-hr-}^\circ\text{R}$$

In view of the uncertainty in calculating the heat transfer coefficient h_T for a fin tube bank, h_T will be taken to be equal to h_F. This is partially justified by the fact that the total fin area is an order of magnitude greater than the total tube area exposed to the air. Thus,

$$h_T = 7.9 \text{ Btu/hr-ft}^2\text{-°R}$$

An estimate of the fin efficiency η_F can be inferred from the solution for heat conduction in a circular fin of rectangular profile attached to a circular tube if the equivalent diameter of the circular fin is taken to be the distance between centers of the heat exchanger tubes. This is a solution given in many elementary texts on heat transfer. From the numerical results given in Ref. 7, it can be estimated that

$$\eta_F = 0.9$$

Taking the conductivity of the brass tubes to be 35 Btu/hr-ft-°F and substituting the appropriate dimensions and heat transfer coefficients into Eqs. (III-4) and (III-5) give

$$U_T = 7.84 \text{ Btu/hr-ft}^2\text{-°F}$$

and

$$U_F = 3.3 \text{ Btu/hr-ft}^2\text{-°R}$$

There are 684 tubes in the heat exchanger and a total 1855 ft^2 of fin surface area; thus

$$W_T = 9.1 \text{ ft}^2/\text{ft}$$

and

$$W_F = 169 \text{ ft}^2/\text{ft}$$

It follows that

$$(T_{b_2} - T_s) = (T_{b_1} - T_s) \exp\left[-\frac{6904 \text{ Btu/hr-°F}}{GC_p}\right]$$

The left-hand side of this expression gives the difference between the temperature of the air leaving the heat exchanger and the steam temperature. The rate of mass flow through the heat exchanger is governed by the total pressure, total temperature, nozzle exit area, and Mach number in the test section.

APPENDIX IV
AN ANALYSIS OF A SELF-ASPIRATING THERMOCOUPLE PROBE

The temperature indicated by a thermocouple probe at steady state is governed by a balance between the conduction, convection, and radiation modes of heat transfer at the thermocouple junction. The complexity of the flow around the thermocouples in the probes (Fig. 1) makes it impossible to analyze them in a rigorous manner and to predict their recovery characteristics theoretically. However, it was found that a reasonably good semi-empirical correlation of the recovery temperature correction can be made. The correlating parameters are derived below. Radiation heat transfer to the thermocouple junction in a self-aspirating probe of the type shown in Fig. 1 may be neglected in comparison with the other two modes of heat transfer. If there were no heat conduction down the thermocouple leads to the stem, the junction temperature (T_{p_a}) would approach the total temperature of the gas (T_o) since the Mach number in the shield (M_s) is always small. Since there is conduction down the leads, however, the equilibrium temperature of the junction will lie between the total temperature of the gas and a temperature, T_{TB} say, characterizing the temperature in the region where the thermocouple leads enter the stem.

From a dimensional analysis, it follows that $(T_{p_a} - T_o)/(T_{TB} - T_o)$ should be a function of only the parameter $\bar{h}\ell/\bar{k}$ where $\bar{h}$ is the average convective heat transfer coefficient for the thermocouple, $\bar{k}$ is an effective thermal conductivity of the thermocouple leads, and ℓ is a characteristic dimension of the thermocouple junction. The smallness of the thermocouple wire and velocity inside the shield yields a low Reynolds number and laminar flow over the thermocouple. It is well known that the Nusselt modulus for heat transfer in laminar flow varies as the square root of the Reynolds number and the cube root of the Prandtl number for body shapes ranging from the flat plate to the sphere. It is, therefore, not unreasonable to assume that this dependence holds for the Nusselt modulus of the thermocouple. Thus,

$$N_{u_l} = \frac{\bar{h}\ell}{\bar{k}} = \alpha \frac{k_a}{\bar{k}} \sqrt{\frac{p_o \gamma \ell M_s}{\sqrt{\gamma R T_o}\,\mu_a}} \sqrt[3]{Pr} \qquad \text{(IV-1)}$$

where α is a constant of proportionality and the gas properties are evaluated at the total conditions of the free stream.

An estimate of the Mach number inside the shield can be obtained by assuming that the flow expands isentropically to the free-stream static pressure at the vent holes. It follows that

$$M_S = C_D \frac{A_v}{A_s} \frac{p}{p_o} \sqrt{\frac{T_o}{T}}\, M \qquad \text{(IV-2)}$$

where C_D is the discharge coefficient for the vent holes. The discharge coefficient for a sharp-edged orifice is approximately constant with a value of 0.6 for a Reynolds number greater than 15 based on orifice diameter. Although the flow situation for the vent holes is somewhat different than the usual orifice flow situation, it is probably sufficiently accurate to take $C_D = 0.6$ in Eq. (IV-2). The vent hole-to-shield ratio for the probe shown in Fig. 1a is approximately 0.183. The internal shield Mach number (M_S) is plotted versus M in Fig. 7. Although $\bar{k}$ and ℓ are unknown, they are fixed for a given probe. It is convenient to combine α, $\bar{k}$, and ℓ into a single dimensional constant $\alpha\sqrt{\ell}/\bar{k}$. Because the exact value of this constant is unimportant in the correlation, it was chosen to make $\bar{h}\ell/\bar{k}$ equal to unity when $p_o = 1$ atm, $T_o = 670°R$, and $M = 1.0$. From Fig. 7, it can be determined that $M_S = 0.0635$ when $M = 1.0$. Hence, $\alpha\sqrt{\ell}/\bar{k} = 1.1 \times 10^4$ ft$^{3/2}$-hr-°R/Btu.

Since the stem temperature (T_{BT}) is unknown, $(T_{p_a} - T_o)/(T_{BT} - T_o)$ cannot be correlated directly with $\bar{h}\ell/\bar{k}$. Both experiment and theory indicate that the recovery temperature for a wide range of geometrical shapes does not depend on Reynolds number except during the transition from laminar to turbulent flow. Therefore, it is not without justification to assume that T_{BT} is independent of Reynolds number. It should be remarked that the stem length was many stem diameters long and that a calculation based on theory of heat conduction in extended surfaces showed stem conduction to be negligible. It follows that, at a given Mach number and total pressure,

$$\frac{\Delta}{\Delta_{ref}} = \frac{f[\bar{h}\ell/\bar{k}]}{f[(\bar{h}\ell/\bar{k})_{ref}]} \qquad \text{(IV-3)}$$

where the subscript ref refers to values of Δ and $\bar{h}\ell/\bar{k}$ at the given Mach number and a reference total pressure.

Figure 8 shows Δ/Δ_{ref} versus $\bar{h}\ell/\bar{k}$ for the data given in Table I for a reference total pressure of 1 psia. The values of Δ_{ref} were obtained from the curve given in Fig. 9, which was obtained by drawing a smooth curve through the average recovery correction for the three probes at 1 psia. The smooth curve in Fig. 8 was taken to represent the data

plotted in Fig. IV-1. From Fig. 8, it can be noted that Δ/Δ_{ref} shows a weak dependence on $\bar{h}\ell/\bar{k}$ at small values of $\bar{h}\ell/\bar{k}$. Thus to a good approximation Δ/Δ_{ref} can be correlated in terms of $\bar{h}\ell/\bar{k}$ alone; that is, the variation with $(\bar{h}\ell/\bar{k})_{ref}$ can be neglected.

In order to obtain Δ from the correlation, Δ_{ref} is obtained from Fig. 9 and Δ/Δ_{ref} is obtained from the smooth curve in Fig. 8. The product of Δ_{ref} and Δ/Δ_{ref} is, of course, Δ. The dashed curves shown in Fig. 5 were obtained in this way. It can be seen that the correlation is reasonably good over the entire range of total pressure and Mach number considered.

It is instructive to consider the effect of total temperature on the recovery correction factor as predicted by the correlation. By assuming that the viscosity and the thermal conductivity of air vary as the 0.7 power of the absolute temperature, it follows that

$$\frac{\bar{h}\ell}{\bar{k}} \propto (T_o)^{0.1}$$

Clearly, changing T_o by any reasonable amount would influence Δ very little. It would be desirable to conduct experiments over a range of temperature to confirm this conclusion.

In order to obtain further confidence in the correlation technique, the data for the self-aspirating probe (Fig. 1c) presented in Ref. 4 were correlated, and the results of the correlation are presented in Fig. IV-2. The correlation is good for the NACA probe. It should be remarked that the correlation curves given in Figs. 7, 8, and 9 are not applicable to the NACA probe because the curves were obtained specifically from the recovery correction data on the probe of the present study. The corresponding correlation curves for the NACA probe were found to differ considerably from the curves in Figs. 7, 8, and 9.

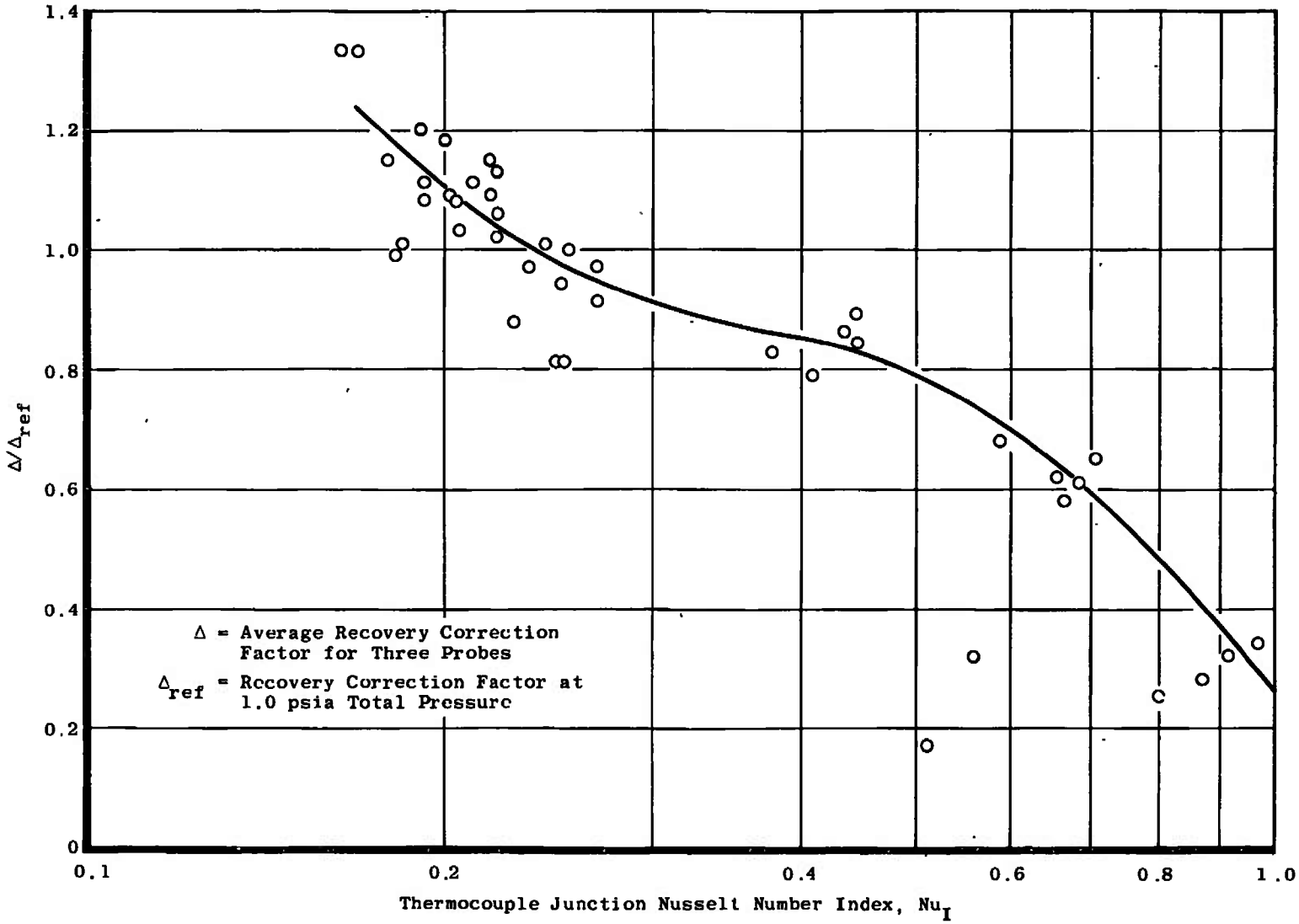

Fig. IV-1 Recovery Correction Factor Ratio versus Nusselt Number Index

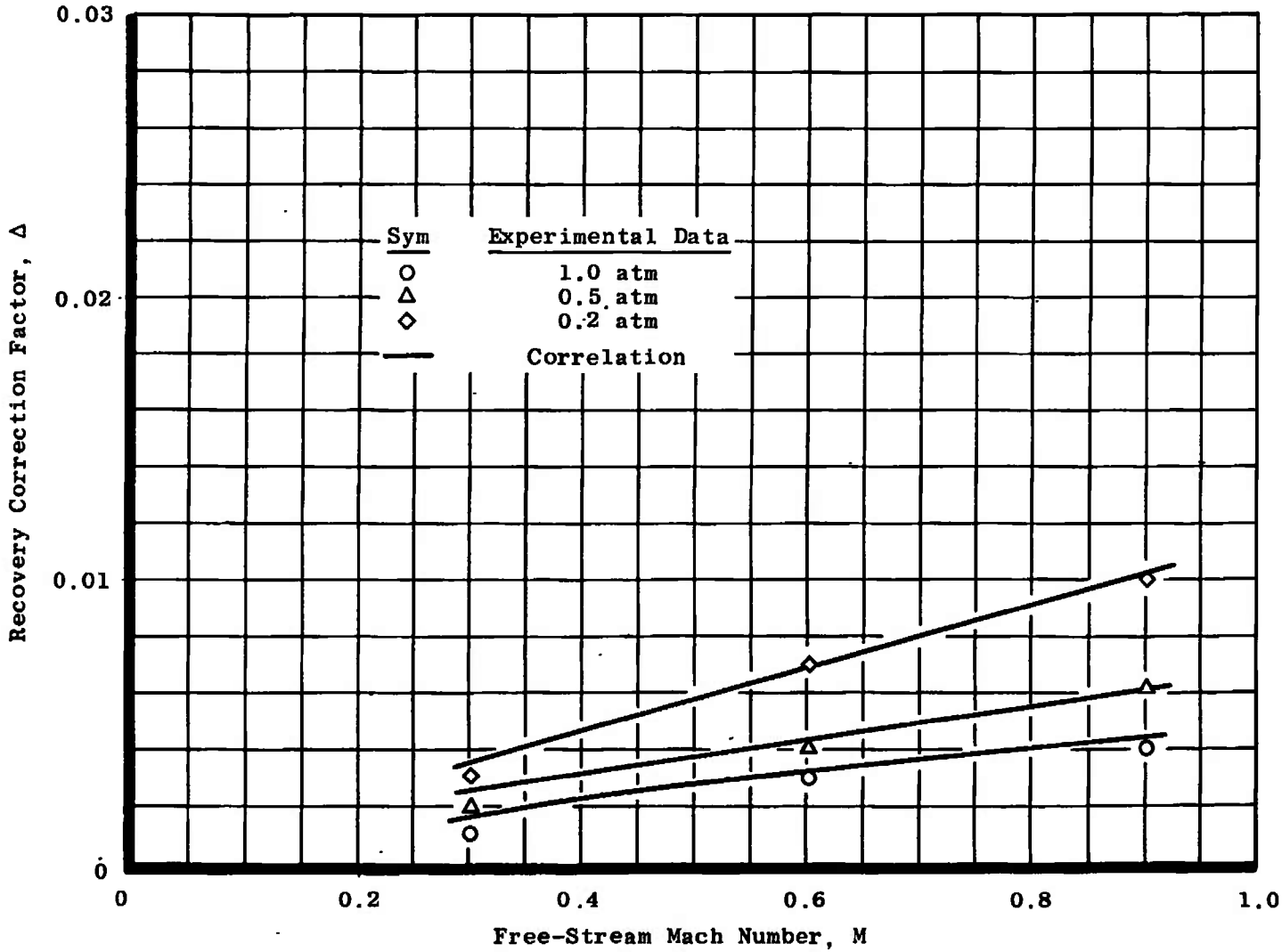

Fig. IV-2 Recovery Correction Factor for NACA Probe (Probe 6, Ref. 4)

UNCLASSIFIED

Security Classification

DOCUMENT CONTROL DATA - R & D

(Security classification of title, body of abstract and indexing annotation must be entered when the overall report is classified)

1. ORIGINATING ACTIVITY *(Corporate author)*
Arnold Engineering Development Center, ARO, Inc., Operating Contractor, Arnold Air Force Station, Tennessee 37389

2a. REPORT SECURITY CLASSIFICATION
UNCLASSIFIED

2b. GROUP
N/A

3. REPORT TITLE
RECOVERY CHARACTERISTICS OF A SINGLE-SHIELDED SELF-ASPIRATING THERMOCOUPLE PROBE AT LOW PRESSURE LEVELS AND SUBSONIC SPEEDS

4. DESCRIPTIVE NOTES *(Type of report and inclusive dates)*
September 1968 to June 1970--Final Report

5. AUTHOR(S) *(First name, middle initial, last name)*
C. E. Willbanks, ARO, Inc.

6. REPORT DATE	7a. TOTAL NO. OF PAGES	7b. NO. OF REFS
April 1971	52	7

8a. CONTRACT OR GRANT NO.	9a. ORIGINATOR'S REPORT NUMBER(S)
F40600-71-C-0002 Program Element 65401F	AEDC-TR-71-68
	9b. OTHER REPORT NO(S) *(Any other numbers that may be assigned this report)* ARO-ETF-TR-71-14

10. DISTRIBUTION STATEMENT Distribution limited to U. S. Government agencies only; covers the test and evaluation of military hardware; April 1971; other requests for this document must be referred to AFAPL (APTP), Wright-Patterson AF Base, Ohio 45433, or AEDC (XON), Arnold AF Stn, Tenn. 37389

11. SUPPLEMENTARY NOTES	12. SPONSORING MILITARY ACTIVITY
Available in DDC	Air Force Aerospace Propulsion Laboratory, Air Force Systems Command, Wright-Patterson AF Base, Ohio 45433

13. ABSTRACT

An apparatus which produces a well-defined flow field for calibration of thermocouple probes over a wide range of subsonic flow conditions at low pressure levels is described. Results for calibration of a typical thermocouple probe used in engine testing are presented. Temperature recovery characteristics are presented for a thermocouple probe of the single-shielded, self-aspirating type for total pressures of 0.75, 1.0, 3.0, 7.5, and 15 psia with subsonic flow speeds ranging from Mach number 0.25 to Mach number 1.0. The total temperature of the air was approximately 670°R for all the tests. An analysis of the probe recovery characteristics based on a semi-empirical correlation was made, and the correlation appears to give satisfactory results over the entire Mach number and total pressure range considered.

Distribution limited to U. S. Government agencies only; other requests for this document must be referred to AFAPL (APTP), Wright-Patterson Air Force Base, Ohio 45433, or AEDC (XON), Arnold Air Force Station, Tennessee 37389.

DD FORM 1 NOV 65 1473

UNCLASSIFIED

Security Classification

14. KEY WORDS	LINK A		LINK B		LINK C	
	ROLE	WT	ROLE	WT	ROLE	WT
thermocouples						
temperature measuring instruments						
probes						
temperature measurements						
test facilities						
subsonic flow						

AFSC
Arnold AFS Tenn